

**NANOPARTICLES OF BIODEGRADABLE POLYMERS
FOR DELIVERY OF THERAPEUTIC AGENTS AND
DIAGNOSTIC SENSITIZERS
TO CROSS THE BLOOD BRAIN BARRIER (BBB) FOR
CHEMOTHERAPY AND MRI OF THE BRAIN**

CHEN LIRONG
(B.Sc)

**A THESIS SUBMITTED
FOR THE DEGREE OF MASTER OF SCIENCE
GRADUATE PROGRAM IN BIOENGINEERING
NATIONAL UNIVERSITY OF SINGAPORE**

2005

ACKNOWLEDGEMENTS

The completion of this project would not have been possible without the help and support from many. I would like to thank the following people for their great contributions to my M.Sc. research.

- My supervisor Prof. Feng Si-Shen and co-supervisor Prof. Sheu Fwu-Shan for their careful and enthusiastic guidance and assistance in my project.
- Professor Wang Shih-Chang and Dr Shuter Borys, Department of Diagnostic Radiology, National University Hospital for their great help in MRI work.
- My fellow colleagues, Dong Yuancai, Khin Yin Win, Yu Qianru, Zhang Zhiping, and Zhou Hu. They have offered me enormous helps in the project.
- Graduate Program in Bioengineering and The Division of Bioengineering, National University of Singapore for the postgraduate scholarship.
- My family and my husband Jiang Xuan. They have been encouraging and supporting me all along.

TABLE OF CONTENTS

ACKNOWLEDGEMENTS	i
TABLE OF CONTENTS	ii
SUMMARY	v
NOMENLCATURE	vii
LIST OF FIGURES	viii
LIST OF TABLES	x
CHAPTER ONE: INTRODUCTION	1
1.1 BLOOD BRAIN BARRIER	1
1.1.1 History and Anatomy of the Blood Brain Barrier	1
1.1.2 Functions of the Blood Brain Barrier	4
1.1.3 Clinical Significance of the Blood Brain Barrier	6
1.2 METHODS TO OVERCOME THE BLOOD BRAIN BARRIER	7
1.3 NANOPARTICLES TO CROSS THE BLOOD BRAIN BARRIER	10
1.4 RESEARCH OBJECTIVES	11
1.4.1 <i>In Vitro</i> Evaluation of PLGA Nanoparticles for Paclitaxel Delivery Across the Blood Brain Barrier	13
1.4.2 Gd-DTPA Loaded Nanoparticles of Biodegradable Polymers for MRI of the Brain	15
1.5 THESIS ORGANIZATION	16
CHAPTER TWO: LITERATURE REVIEW	17
2.1 CANCER, CHEMOTHERAPY, AND CONTROLLED DRUG DELIVERY	17
2.2 BRAIN CANCER AND OTHER BRAIN DISEASES	20
2.3 NANOPARTICLE TECHNOLOGY	21
2.3.1 Introduction of Nanoparticles	21
2.3.2 Fabrication techniques of Nanoparticles	22
2.3.2.1 Dispersion of performed polymers	22

2.3.2.2 Polymerization methods	24
2.4 BIODEGRADABLE POLYMERS IN CONTROLLED DRUG DELIVERY	25
2.4.1 Biodegradable Polymers in Drug Delivery Systems	25
2.4.2 Poly(lactide-co-glycolide) (PLGA)	28
2.4.3 Poly(Lactic acid)-poly(ethylene glycol) (PLA-PEG) Copolymers	29
2.5 NANOPARTICLES OF BIODEGRADABLE POLYMERS TO PENETRATE THE BLOOD BRAIN BARRIER	30
2.5.1 Ideal Properties of Nanoparticles across the Blood Brain Barrier	30
2.5.2 Possible Mechanism of Nanoparticles to Penetrate the Blood Brain Barrier	31
2.5.3 Surface Modification of Nanoparticles	33
2.6 MRI AND MRI CONTRAST MEDIUM	34
CHAPTER THREE: MATERIALS AND METHODS	36
3.1 MATERIALS	36
3.2 METHODS	37
3.2.1 <i>In Vitro</i> Evaluation of PLGA Nanoparticles for Paclitaxel Delivery Across the Blood Brain Barrier	37
3.2.1.1 Fabrication of nanoparticles	37
3.2.1.2 Nanoparticles characterizations	37
3.2.1.3 Encapsulation efficiency of paclitaxel	38
3.2.1.4 <i>In vitro</i> release of paclitaxel	39
3.2.1.5 Cell culture and cellular uptake experiments	40
3.2.2 Gd-DTPA Loaded Nanoparticles of Biodegradable Polymers for MRI of the Brain	41
3.2.2.1 Fabrication of nanoparticles	41
3.2.2.2 Encapsulation efficiency of Gd-DTPA	42
3.2.2.3 <i>In vitro</i> release of gadolinium	42
3.2.2.4 <i>In vitro</i> and <i>in vivo</i> MRI	42
CHARPTEER FOUR: RESULTS AND DISCUSSION	44
4.1 <i>IN VITRO</i> EVALUATION OF PLGA NANOPARTICLES FOR PACLITAXEL	44

DELIVERY ACROSS THE BLOOD BRAIN BARRIER	
4.1.1 Particle Size and Size Distribution	44
4.1.2 Zeta Potential	48
4.1.3 Drug Loading and Drug Encapsulation Efficiency (EE) of Paclitaxel	50
4.1.4 Morphology	54
4.1.5 In Vitro Release of Paclitaxel	57
4.1.6 Cell Culture	59
4.1.7 Cellular Uptake of Nanoparticles	61
4.2 GD-DTPA LOADED NANOPARTICLES OF BIODEGRADABLE POLYMERS FOR MRI OF THE BRAIN	65
4.2.1 Particle Size	65
4.2.2 Morphology	67
4.2.3 Loading and Encapsulation Efficiency of Gadolinium	69
4.2.4 <i>In Vitro</i> Release of Gadolinium	71
CHAPTER FIVE: CONCLUSIONS AND FUTURE WORK	73
5.1 CONCLUSION	73
5.2 FUTURE WORK	74
REFERENCE	75
PUBLICATION LIST	82

SUMMARY

Blood brain barrier (BBB) was first discovered by Dr. Paul Enrilich in the late 19th century. It is a physiological barrier existing for molecular transportation between the blood and the central nervous system (CNS). BBB plays an important role in maintaining a homeostatic environment for a healthy and efficient brain and protecting the brain from harmful chemicals. However, it is considered to be the main obstacle for a large number of drugs to enter the brain. Nanoparticles provide a feasible choice as a drug delivery device to cross the BBB because it may overcome the biological barrier and increase the bioavailability of the drug in the brain and CNS.

The aim of this thesis is to develop nanoparticles of biodegradable polymers for drug delivery across the blood brain barrier. Emphasis is given to investigate the possible effects of the particle surface coating. The work can be divided into two parts. In the first part, poly(lactic-co-glycolic acid) (PLGA) nanoparticles were prepared by a modified single emulsion solvent evaporation method. Anti-cancer drug paclitaxel or fluorescent marker coumarin-6 was encapsulated in the PLGA nanoparticles. PVA and Vitamin E TPGS were used as emulsifiers. Tween 80, poloxamer 188 and poloxamer 477 were used as coating materials to modify the surface of the nanoparticles. Nanoparticles of various recipes were characterized by various state-of-the-art techniques. A model cell line, Madin-Darby Canine Kidney (MDCK) cell line, was used to simulate BBB to investigate the feasibility of the nanoparticles to cross the blood brain barrier as well as the effects of the surface coating. *In vitro* uptake of fluorescent nanoparticles by MDCK cells was evaluated qualitatively by

microreader and quantitatively by confocal laser scanning microscopy. In cellular uptake experiments of nanoparticles, it was found that all the nanoparticles can be internalized by the MDCK cells to certain extent and the percentage of the cellular uptake of the nanoparticles was highly affected by the surface coating. It was thus concluded that it is feasible for nanoparticles of biodegradable polymers to deliver drugs across the blood brain barrier and the surface coating plays key roles in determining the extent of the particles to cross the BBB.

To further investigate the potential for the nanoparticles to cross the BBB, animal testing is important and necessary. The second part of the thesis is thus focused on a feasibility investigation for polymeric nanoparticles to deliver contrast materials across the BBB for brain image. Gadolinium-DTPA(Gd-DTPA) loaded PLGA or poly(Lactic acid)- poly(ethylene glycol) (PLA-PEG) nanoparticles were made by the nanoprecipitation and *in vivo* animal investigation was carried out to evaluate the effects of surface coating on magnetic resonance imaging (MRI). It was found that PLA-PEG nanoparticles of size less than 100 nm and PLGA nanoparticles of diameter less than 200 nm can be manufactured by the nanoprecipitation method. 0.92-1.74% loading of Gd-DTPA was obtained in the particles. *In vivo* MRI is still under development.

NOMENCLATURE

BBB	Blood brain barrier
DCM	Dichloromethane
DMEM	Dulbecco's modification of Eagle's medium
EE	Encapsulation efficiency
Gd-DTPA	Gadolinium DTPA
HBSS	Hank's balanced salt solution
HPLC	High performance liquid chromatography
ICP-AES	Inductively Coupled Plasma - Atomic Emission Spectrometer
MDCK	Madin-Darby canine kidney
MDR	Multidrug resistance
MRI	Magnetic Resonance Imaging
MRP	Multidrug resistance protein
P-gp	P-glycoprotein
PLA-PEG	Poly (Lactic acid) - poly(ethylene glycol)
PLGA	Poly (D, L-lactide-co-glicolide)
PVA	Polyvinyl alcohol
Vitamin E TPGS	vitamin E succinate with polyethylene glycol 1000

LIST OF FIGURES

Fig.1 The blood brain barrier

Fig. 2 The BBB as an impermeable wall.

Fig. 3 The BBB as a selective sieve.

Fig. 4 Chemotherapy cycles

Fig. 5 Drug levels in the blood with (Left) traditional drug dosing and (Right) controlled delivery dosing

Fig. 6 Chemical structure of Gd-DTPA

Fig. 7 Chemical structure of PVA and VE-TPGS

Fig. 8 Encapsulation efficiency of the nanoparticles. Sample 1 is PVA emulsified nanoparticles. Sample 5 is TPGS emulsified nanoparticles.

Fig. 9 Chemical structure of paclitaxel

Fig. 10 Drug content of the nanoparticles.

Fig. 11 SEM and AFM images of the nanoparticles (from top to bottom: Sample 1, PVA emulsified nanoparticles; sample 2, PVA emulsified Tween 80 coated nanoparticles; sample 3, PVA emulsified poloxamer 188 coated nanoparticles; sample 4, PVA emulsified poloxamer 407 nanoparticles; sample 5, TPGS emulsified nanoparticles).

Fig. 12 The release profile of paclitaxel from the nanoparticles in PBS

Fig. 13 Morphology of MDCK cells at low density (left) and high density (right).

Fig. 14 Morphology of bovine brain microvascular endothelial cells (BBMVEC)

Fig. 15 Cellular uptake of nanoparticles in MDCK cells

Fig. 16 Confocal laser scanning microscope images of PLGA nanoparticles internalized in MDCK cells (Sample 1,PVA emulsified nanoparticles; sample 2, PVA emulsified Tween 80 coated nanoparticles; sample 3, PVA emulsified poloxamer 188 coated nanoparticles; sample 4, PVA emulsified poloxamer 407 nanoparticles; sample 5, TPGS emulsified nanoparticles)

Fig. 17 SEM image of PLGA nanoparticle

Fig. 18 SEM image of PLA-PEG nanoparticles

Fig. 19 Release of gadolinium from the nanoparticle

LIST OF TABLES

Table 1 Drug delivery to CNS: technical approaches, advantages and limitations

Table 2 Structures of biodegradable polymers usually used in drug delivery.

Table 3 Ideal properties of polymeric-based nanoparticles for drug delivery across the BBB.

Table 4 Size and size distribution of different nanoparticles.

Table 5 Zeta potential of different nanoparticles

Table 6 The size and polydispersity of the Gd-DTPA loaded particles

Table 7 Encapsulation efficiency and drug content of the Gd-DTPA loaded nanoparticles

CHAPTER ONE

INTRODUCTION

1.1 BLOOD BRAIN BARRIER

Blood brain barrier (BBB) exists between the blood and the central nervous system (CNS), which is a physiological barrier for molecular transportation between the blood and the CNS. It provides neurons with precisely controlled nutritional requirements to maintain a proper balance of ions and other chemical constituents and isolate the central nervous systems from toxic chemicals in the blood.

1.1.1 History and Anatomy of Blood Brain Barrier

It was in the late 19th century that the concept of blood-brain barrier arose. The German bacteriologist Paul Ehrlich, the 1908 Nobel Laureate of Medicine and the Father of Chemotherapy, observed that certain dyes, e.g., a series of aniline derivatives, administered intravenously to small animals, stained all the organs except for the brain [1]. In subsequent experiments, Edwin E. Goldmann, a student of Ehrlich, injected the dye trypan blue directly into the cerebrospinal fluid of rabbits and dogs. He found that the dye readily stained the entire brain but did not enter the blood stream to stain the other internal organs [2]. The observations drawn from the dye studies indicated that the central nervous system is separated from the blood system by a barrier of some kind. Lewandowsky, while studying potassium ferrocyanide

penetration into the brain, was the first to coin the term blood-brain barrier and called it "bluthirnschranke" [3].

In the 1960s, Reese and Karnovsky [4] and Brightman and Reese [5] repeated the Ehrlich/Goldmann experiments at the ultrastructural level by using electron microscopy to observe the distribution of the protein tracer horseradish peroxidase following intravenous or intrathecal administration. These experiments conclusively identified the brain capillary endothelial cell as the site of the brain blood barrier.

Later experiments demonstrated that the BBB is composed of epithelial tight junctions between the plasmalemma of adjacent cells in cerebral capillaries and is surrounded by astrocyte foot process [5, 6]. Fig. 1 below shows the diagram of the blood brain barrier in detail. The brain capillary is lined with a layer of special endothelial cells that lack fenestrations and is sealed with tight junctions.

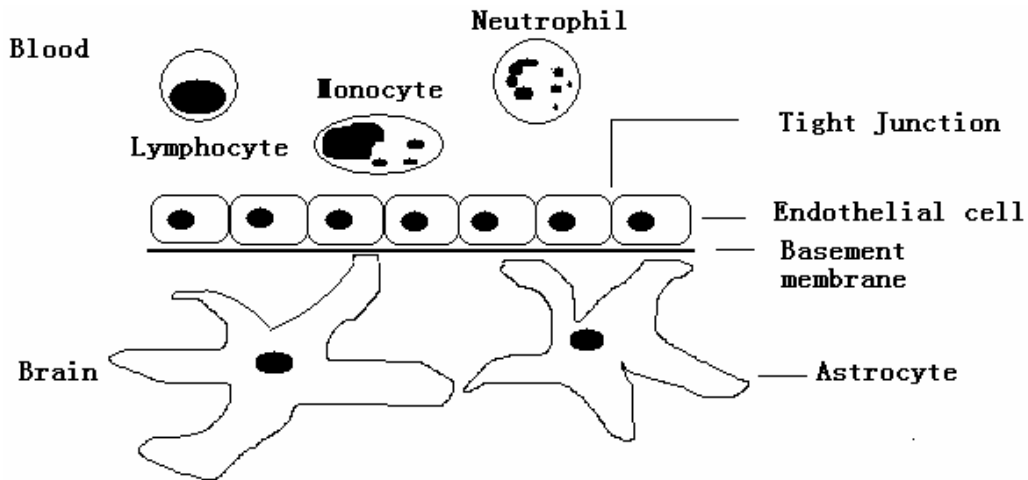


Fig 1 The blood brain barrier

The tight junctions between endothelial cells results in a very high transendothelial electrical resistance of 1500-2000 $\Omega\cdot\text{cm}^2$ compared to 3-33 $\Omega\cdot\text{cm}^2$ of other tissues which reduces the aqueous based paracellular diffusion that is observed in other organs [7, 8]. The normal blood brain barrier restricts trans- and paracellular movement of blood-born molecules, effectively filtering most ionized, water-soluble molecules greater than 180 Daltons in mass [9, 10]. In the case of brain tumor, the blood brain barrier is frequently not intact in the center of the malignantly as demonstrated by computerized tomography and MR imaging [9]. However, the presence of an intact blood brain barrier at the proliferating edge of the tumor has been suggested to be one of the major contributing factors to the failure of chemotherapy in the treatment of central nervous system neoplasms [11, 12].

Comparing brain and general capillaries, brain capillaries are structurally different from the blood capillaries in other tissues, which result in the properties of the blood brain barrier. Brain capillaries lack the small pores that allow rapid movement of solutes from circulation into other organs. In brain capillaries, intercellular cleft, pinocytosis, and fenestrae are virtually nonexistent; exchange must pass transcellularly. Therefore, only lipid-soluble solutes that can freely diffuse through the capillary endothelial membrane may passively cross the BBB. In capillaries of other parts of the body, such exchange is overshadowed by other nonspecific exchanges. Moreover, there are astrocytes foot processes or limbs that spread out and abutting one other, encapsulate the capillaries closely associated with the blood vessels to form the BBB.

Recent progress in molecular biology revealed that multi-drug efflux pump proteins such as P-glycoproteins (p-gp), multidrug resistance protein (MRP) are rich in the brain capillaries endothelial cell membrane, which may also play a key role to constitute the BBB. These proteins are active transport systems responsible for outward transport of a wide range of substances [13]. Both P-gp and MRP are membrane proteins belonging to the ABC (ATPbinding cassette) transport protein family and can confer multidrug resistance (MDR). They are energy-dependent pumps located in the BBB, sharing some functional similarities (somewhat overlapping substrate specificities) with broad substrate specificity. Evidence shows that P-gp excludes a number of lipophilic compounds from cerebral endothelial cells [14]. Many MRP substrates are amphiphilic anions with at least one negatively charged group although MRP can also transport cationic and neutral compounds. It appears that there are two mechanisms for transport of MRP substrates dependent on their ionic nature: direct transport of anionic compounds, whereas, for some cationic and neutral compounds the presence of glutathione, likely via cotransport, is required [13].

1.1.2 Functions of the Blood Brain Barrier

The main function of the blood brain barrier is to protect the brain. The BBB serves as an impermeable wall to prevent the entry of agents from outside of the brain [15]. It has been identified that the brain capillary endothelial cell as the physical site of the BBB. The continuous tight junctions that seal together the margins of the endothelial cells play very important roles in forming the blood brain barrier. Furthermore, in

contrast to endothelial cells in many other organs, brain capillary endothelial cells contain no direct transendothelial passageways such as fenestrations or channels.

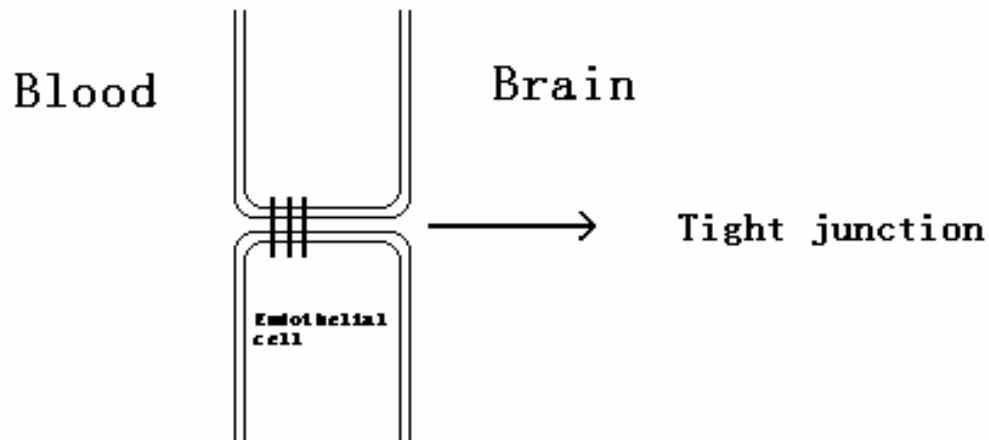


Fig 2 The BBB as an impermeable wall.

However, the blood brain barrier cannot be absolute. It must facilitate the exchange of selected solutes to deliver metabolic substrates and remove metabolic wastes. Therefore, the blood brain barrier also serves as a selective sieve [15]. Lipid-soluble fuels and waste products, such as O₂ and CO₂, can readily cross the lipid bi-layer membranes of the endothelial cell and, thus, encounter little difficulty in quickly exchanging of metabolic molecules between blood and brain. Polar solutes such as glucose and amino acids, however, must depend on other mechanisms to facilitate their exchange. This is accomplished by the presence of specific, carrier-mediated transport proteins in the luminal and abluminal membranes of the brain capillary endothelial cell.

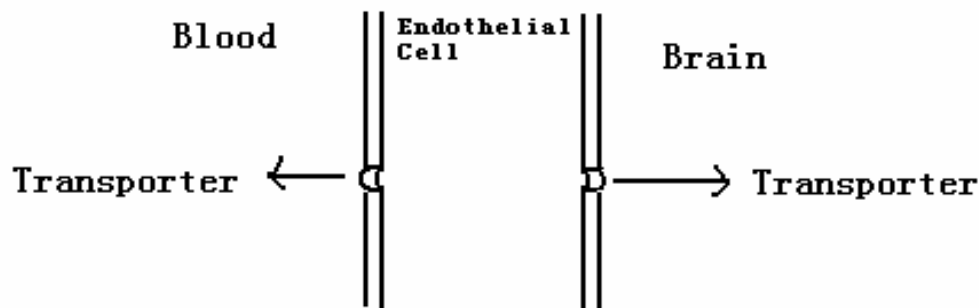


Fig 3 The BBB as a selective sieve.

With these two functions of the blood brain barrier, the brain capillaries allow the passage of oxygen and other essential chemicals and shield the brain from toxins in the circulatory system and from biochemical fluctuations and, consequently provide a safe environment to the brain.

1.1.3 Clinical Significance of the Blood Brain Barrier

Blood brain barrier serves to protect the brain from toxic agents. However, it also becomes an insurmountable obstacle for a large number of drugs. Almost all of the lipophilic anticancer agents such as doxorubicin [16, 17], epipodophylotoxin and vinca alkaloids [18] hardly enter the brain. As a consequence, the therapeutic value of many promising drugs is diminished, and brain tumors and other CNS diseases such as alzheimer's disease [19], Parkinson's disease [20] and HIV infection [21] have proved to be most refractory to therapeutic interventions. There are twice as many people suffering from central nervous system diseases as those suffering from

diseases of the blood vessels and heart. However, the world-wide CNS drug market is US\$33 billion, which is only half of the size for the latter diseases [22]. This is all because of the blood brain barrier. For all these diseases that occur in the central nervous systems, the biggest problem is how to overcome the blood brain barrier.

1.2 METHODS TO OVERCOME THE BLOOD BRAIN BARRIER

To solve the problems encountered in treatment of brain diseases, a lot of efforts have been made and various strategies for enhanced CNS drug delivery have been proposed [8, 23-27]. These strategies can be divided into three categories: manipulating drugs, disrupting the blood brain barrier and finding alternative routes for drug delivery. Drug manipulation includes lipophilic analogs [28], prodrugs [29-31], chemical drug delivery [32, 33], carrier-mediated drug delivery [34], and receptor/vector mediated drug delivery [35-39]. Disturbing the blood brain barrier includes osmotic blood brain barrier disruption [40-44] and biochemical blood brain barrier disruption [45-47]. Alternative routes to CNS drug delivery include intraventricular/intrathecal route [48], and olfactory pathway [49-51]. Besides these methods, there were some direct ways of circumventing the BBB. That is to deliver drugs directly to the brain interstitium, which includes injections, catheter, and pumps [52, 53]; biodegradable polymer wafers [54, 55], microspheres and nanoparticles; and drug delivery from biological tissues [56].

Table 1 shown below summarizes the technical approaches, their advantages and limitations.

Table 1 Drug delivery to CNS: Technical approaches, advantages and limitations [19].

Technical approach	Advantages	Limitations
Non-invasive		
Lipophilic analog	Readily penetrate CNS e.g. Heroin and analogues of nitrosoureas Delivered without disulfide or ester linkages, which affect pharmacological actions	Poor aqueous solubility, limit to 400-600 dalton molecular weight for BBB threshold, enhanced peripheral distribution
Liposomes/PEGylated immunoliposomes	Capable of receptor-mediated transport through the BBB in-vivo	Do not undergo significant transport through the BBB in the absence of vector-mediated drug delivery
Prodrug	High drug residence time e.g, Fatty acid, glyceride or phospholipids precursors of levodopa, GABA, Niflumic acid, valproate or vigabatrin and suitable for specific membrane transporter, such as the amino acids, peptide or glucose transporter.	Poor selectivity, poor retention, and the possibility for reactive metabolites. Dose limited toxicity.
Chemical drug delivery	Site-specific drug delivery e.g, neuropeptides	The oxidative lability and the hydrolytic instability combine to limit the shelf-life of the CDs.
Redox chemical delivery systems	Increases intracranial concentrations of a variety of drugs including neurotransmitter, antibiotics, and antineoplastic agents.	
Carrier mediated drug delivery	Controls the delivery and retention of drugs, e.g., Levodopa and melphalin.	Highly stereospecific drug is to be converted into a structure similar to that of an endogenous nutrient.

Receptor/Vector mediated drug delivery	Allows designing transport linker to suit the specific functional needs of the therapeutic agents, includes peptide-based pharmaceuticals and small molecules incorporated without liposomes.	Saturable process, enzymatic dependent release, attachment to a BBB transport vector renders certain drug inactive.
Osmotic blood brain barrier disruption	Alters barrier-inducing factors, e.g., cytotoxic drugs Promising delivery strategy for recombinant adenoviral vector, magnetic resonance imaging agents and macromolecular drugs.	Often leads to unfavorable toxic/ therapeutic ratio and breaks down the self-defence mechanism of the brain
Biochemical blood brain barrier disruption	Selective opening of brain tumor capillaries e.g. intracarotid infusion of leukotriene C4	Breaks down the self-defense mechanism of the brain.
Olfactory Pathway	Direct nose-to-brain transport and access to CSF e.g. neurotropic factors.	Enzymatically active, low PH nasal epithelium, mucosal irritation or variability caused by nasal pathology.
Invasive		
Intraventricular / Intrathecal Route	Bypasses the BCB and results in immediate high CSF drug concentrations, encounter minimized protein binding and decreased enzymatic activity, longer drug half-life.	Slow rate of drug distribution within the CSF and increase in intracranial pressure results into high clinical incidence of hemorrhage, CSF leaks, neurotoxicity and CNS infections.
Injections, Catheters, and Pumps	Continuous drug delivery. Distribution of drugs can be maintained.	Due to diffusion problems, the therapeutic agent is likely to reach only nearby sites.
Biodegradable polymer Wafers,	Circumvent the BBB, controlled drug delivery	Useful in a very limited number of patients.
Microspheres and Nanoparticles	Polymeric cytokine delivery obviating the need for transfecting cytokine genes, produces longer periods of cytokine release in-vivo and yield more reproducible cytokine release	Due to diffusion problems, the therapeutic agents is likely to reach only nearby sites (<1mm).

	profile and total cytokine dose. Easily implantable without damage	General toxic effect is a serious impediment,
Drug Delivery from Biological Tissues	Therapeutic proteins can be released from co-grafted cells	Inefficient transfection of host cells, nonselective expression of the transgene and deleterious regulation of the transgene by the host.

All the methods mentioned above have advantages and limited factors. Among these methods, nanoparticles of biodegradable polymers have shown to be one of the promising strategies.

1.3 NANOPARTICLES TO CROSS THE BLOOD BRAIN BARRIER

Nanoparticles are solid colloidal particles ranging in size from 10 to 1000 nm, in which therapeutic drugs can be adsorbed, entrapped, or covalently attached [57]. Formulated by nanoparticles, drugs can be released at right rate and dose at specific sites in body during a certain time to realize the accurate delivery which will enhance the therapeutic efficacy and reduce the side effects.

The potential advantages of nanoparticles for drug delivery across the BBB include [58]:

1. Nanoparticle system can deliver a relatively more concentrated drug dose to the brain, compared to that for the prodrug or drug-vector approach, reducing the needed dose and thus the drug-associated side effects;

2. Nanoparticles of small enough size may have ability to transport through the tight junction (knealing between endothelial cells, paracellular transportation);
3. Nanoparticles are capable of bypassing the P-gp efflux system. Nanoparticles may be equipped with a mask (surface coating) to the p-gp to bring the drug molecules across the BBB;
4. Nanoparticles may offer protection for the activity of the drug molecules during transportation in the circulation, across the BBB and in the brain;
5. Nanoparticles may provide sustained release of drug in the brain to prolong the pharmacological action of drug molecules;
6. Nanoparticle formulation is a platform technology, which can be applicable to a wide range of drugs, either hydrophilic or lipophilic.
7. Nanoparticles of small enough size and appropriate coating may have ability to escape from the elimination by the RES to realize long-circulating properties,

1.4 RESEARCH OBJECTIVES

Until now, only a few papers have been published on using nanoparticles to deliver across the BBB therapeutic agents for chemotherapy and contrast materials for medical imaging of the brain. However, most of them were focused on using poly(butylcyanoacrylate) (PBCA) nanoparticles with surface coating of polysorbate 80. Despite the success of PBCA nanoparticles for drug/peptide delivery across the BBB, this kind of nanoparticles has its disadvantages. Firstly, this polymer is not

authorized to application in human (not FDA-approved). Secondly, there have been reports of *in vivo* toxicity of PBCA-polysorbate 80 nanoparticles. Olivier et al reported that PBCA nanoparticle caused mortality (3 to 4 out of 10 mice) and dramatically decreased locomotor activity in mice dosed with dalargin loaded PBCA nanoparticles, but not with non biodegradable polystyrene nanoparticles (the latter did not show any CNS penetration of dalargin) [59]. It was concluded by the researchers that a non specific permeabilization of the BBB, probably related to the toxicity of the carrier, may account for the CNS penetration of dalargin associated with PBCA nanoparticles and polysorbate 80. Considering the *in vivo* toxicity reported on the PBCA nanoparticle system, FDA-approved biodegradable polymers such as PLGA and PLA-PEG were used in this project. Our main objective is to developed an appropriate nanoparticle technology to make PLGA and PLA-PEG nanoparticles of small enough size and appropriate surface coating to deliver therapeutic agents and contrast materials across the blood brain barrier for chemotherapy and medical imaging of the brain, respectively. The project can be divided into two parts. In the first part, paclitaxel loaded PLGA nanoparticles will be prepared by a modified single emulsion method and characterized by various state-of-the art techniques. *In vitro* evaluation of such nanoparticles to cross the blood brain barrier will be investigated by employing MDCK cell line as an *in vitro* model of the BBB. The effects of the surface coating will be studied. In the second parts, gadolinium-DTPA loaded PLGA and PEG-PLA nanoparticles will be prepared by the nanoprecipitation method, which will be injected in animals for *in vivo* magnetic resonance imaging (MRI).

1.4.1 *In Vitro* Evaluation of PLGA Nanoparticles for Paclitaxel Delivery Across the Blood Brain Barrier

PLGA is used in this research because of its biodegradability and biocompatibility. It is approved by US Food and Drug Agency (FDA). PLGA nanoparticles were usually prepared in the literature by single emulsion solvent evaporation method with polyvinyl alcohol (PVA), a commercial macromolecule product as the emulsifier [60]. However, despite repeated washing, a fraction of PVA may always remain on the nanoparticle surface because PVA forms an interconnected network with the polymer at the interface [61]. The residual PVA associated with PLGA nanoparticles may have side effects and affect the physical properties and cellular uptake of the nanoparticles. To reduce or remove the negative effects of the residual PVA, surface modification of the particles will be carried out by surface coating or replacing the PVA emulsifier by a natural emulsifier such as phospholipid or PEGylated vitamin E (full name, or Vitamin E-TPGS or TPGS). Three coating materials, Tween 80, poloxamer 188 and poloxamer 407 will be used in the study. These materials are all amphiphilic polymers and may change the hydrophobicity of the particle surface. Tween 80 has been reported to be useful for overcoming the blood brain barrier with PBCA nanoparticles [62, 63-65]. Poloxamers have been reported to help the particles prolong the time in the blood stream by forming a steric stabilizing layer of PEG on the surface of the particle [66, 67]. TPGS has shown to be an effective emulsifier which can achieve high drug encapsulation efficiency, size and size distribution, morphological and physicochemical properties, desired *in vitro* release kinetics of the nanoparticles, and high cellular uptake of nanoparticles [68-71]. In this study the

effects of all these surfactants on the feasibility of nanoparticles to penetrate the blood brain barrier will be investigated.

Paclitaxel (Taxol®) is one of the most potent antitumor agents and has been approved by FDA for treatment of a wide spectrum of cancers, especially breast cancer, ovarian cancer, small cell and non small cell lung cancer [72-76]. It has also been used to treat malignant glioma and brain metastases [77-79]. However, brain tumors constitute a difficult problem and the therapeutic benefit of paclitaxel has been limited. This could be attributed to delivery problem to cross the BBB. Although paclitaxel is very lipophilic, concentrations in the CNS were found very low after intravenous administration [80, 81]. It was demonstrated that the p-gp blocker valsopodar enhances paclitaxel entry into the brains of mice after intravenous dosing and that valsopodar dramatically increases paclitaxel effectiveness against a human glioblastoma implanted into the CNS of nude mice [82]. These represent the preliminary data directly demonstrating the role of p-gp in limiting the therapeutic availability of paclitaxel to the CNS.

In this study, paclitaxel loaded PLGA nanoparticles will be prepared by single emulsion solvent evaporation method. Madin-Darby canine kidney (MDCK) cell line will be used as an *in vitro* model of the BBB. MDCK is a kidney epithelial cell line, which forms a tight monolayer similar to that of the brain endothelial cell monolayer. MDCK cells display morphological and enzymatic characteristics also found in the brain endothelial cells (e.g., acetylcholinesterase, butyryl-cholinesterase, gamma-glutamyl transpeptidase). MDCK monolayer represents a relatively simple model for

the screening of compounds that are transported passively across the blood-brain barrier.

1.4.2 Gd-DTPA Loaded Nanoparticles of Biodegradable Polymers for MRI of the Brain

To further evaluate the potential of nanoparticles of biodegradable polymers to penetrate the BBB, animal study is important and necessary. Radiology agent was usually used to label the nanoparticles in the literature. However, it is not safe. In our study, Gd-DTPA loaded nanoparticles will be prepared to facilitate the visualization of the particles administered in rats. Gd-DTPA is a widely used, commercially available MRI contrast agent. MR imaging is a imaging method using a strong magnetic field and gradient fields to localize bursts of radiofrequency signals coming from a system of spins consisting of reorienting hydrogen H nuclei after they have been disturbed by radiofrequency RF pulses. It can produces detailed pictures of the brain. Thus, *in vivo* study on nanoparticles to cross the blood brain barrier can be carried out by injecting Gd-DTPA loaded nanoparticles intravenously to the animal and then detect the distribution of the nanoparticle by MR. Our objective is to prepare Gd-DTPA loaded PLGA and PEG-PLA nanoparticles by the nanoprecipitation method and investigate its *in vivo* image of the animal brain by MRI. Particle size, surface charge, agent encapsulation efficiency and *in vitro* release of Gd-DTPA will also be studied and compared among nanoparticles of various biodegradable polymer/copolymers to pursue a best nanoparticle formulation.

1.5 THESIS ORGANIZATION

This thesis is made up of five chapters. Chapter One gives a general introduction of the project. It comprises of introduction and clinical significance of the blood brain barrier, a review of various methods to overcome the blood brain barrier, the possibility of nanoparticles of biodegradable polymers to cross the blood brain barrier, as well as the objective of this project. Chapter Two is a collection of summarized information on cancer, chemotherapy, drug delivery, and nanoparticles of biodegradable polymers. In Chapter Three the various materials and methods used in the experiments are reported. The experimental results and discussions are presented in Chapter Four. Finally, the conclusions drawn from the project and the future work are presented in Chapter Five.

CHAPTER TWO

LITERATURE REIVEW

2.1CANCER, CHEMOTHERAPY, AND CONTROLLED DRUG DELIVERY

Cancer is any malignant growth or tumor caused by abnormal and uncontrolled cell division; it may spread to other parts of the body through the lymphatic system or the blood system [83]. There are more than 10 million people diagnosed with cancer every year. Cancer causes 6 million deaths every year— or 12% of deaths worldwide [84]. It is estimated that there will be 15 million new cases every year by 2020. In the United States of America, a quarter of all deaths are due to cancer. It was estimated that 203.1 per 100,000 persons were died of cancer in 1997 and that there were totally 1,334,100 new cancer cases and 556,500 deaths in 2003 [85]. In China, cancer has been the first and second cause of death in urban area (23.89% of total deaths) and rural areas (18.40% of total deaths), respectively [86]. In Singapore, cancer continued to be the leading cause of death in 2001, accounting for 28.2 percent of all deaths [87].

The objectives of cancer treatment are to cure the patients if possible, prolong their life, and improve the quality of their life. Treatment of cancer may involve surgery, radiation therapy, chemotherapy, biotherapy, bone marrow transplant, or some combination of these [88]. Usually surgery is the first treatment for cancers. However, it is difficult for surgical removal of solid tumor to be thorough and it is not

applicable for some cases such as leukemia. It is estimated that more than half of cancer patients receive systemic chemotherapy as part of their treatment [88].

Chemotherapy, at the first point, is to employ chemicals in treatment of diseases. It can be defined as “curing by chemicals” [89, 90]. In chemotherapy, drugs are normally given in cycles, most commonly three to four weeks apart, in a period of four to six months. Between cycles, the normal cells (blue line) recover but the tumor cells (red line) do not (see figure below). Over the entire course it’s hoped that the tumor cells would have been destroyed, leaving the body a little battered but intact.

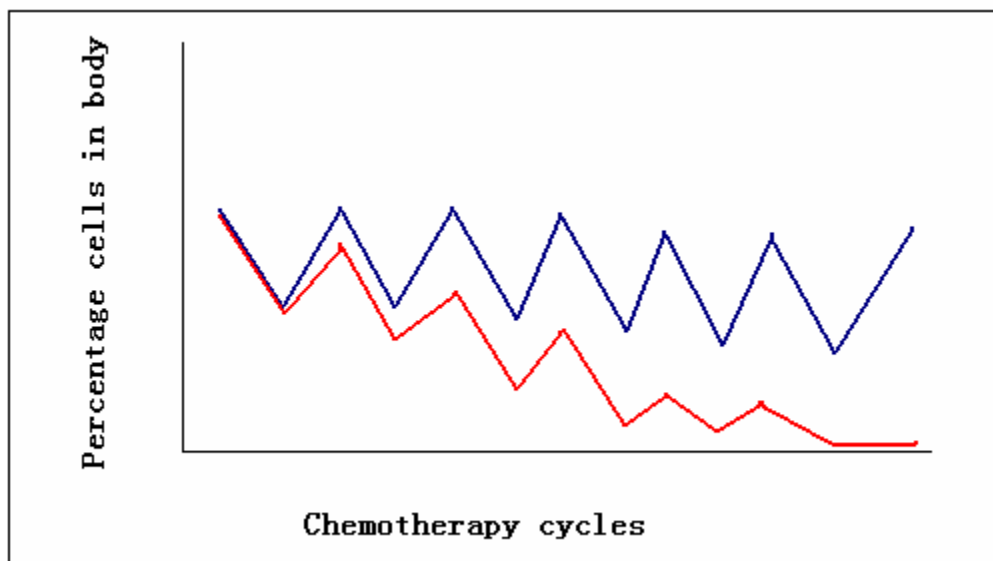


Fig 4 Chemotherapy cycles

The disadvantage of chemotherapy is that normal cells can also be harmed by the anticancer drugs, especially those cells that normally divide quickly. These include cells in the hair follicles, bone marrow, and lining of the gastrointestinal tract. The results can be hair loss; depressed red and white blood cell counts, causing anemia

and an inability to fight off infections, respectively; and nausea, vomiting and mouth sores. Chemotherapy can also have several neurological side effects, such as fuzzy thinking and difficulty concentrating [91].

Controlled drug delivery systems provide an alternative to the traditional chemotherapy, which have several advantages. Controlled drug delivery occurs when a polymer, whether natural or synthetic, is judiciously combined with a drug or other active agent in such a way that the active agent is released from the material in a pre-designed manner [92]. Firstly, controlled drug delivery systems can improve the efficacy of the drug. Secondly, it can reduce toxicity of the cancer drug and side effects of drug adjuvant [93]. Thirdly, it can provide a sustained and effective drug level by controlled release of the drug (Fig. 5). Last but not least, it can improve patient compliance and convenience.

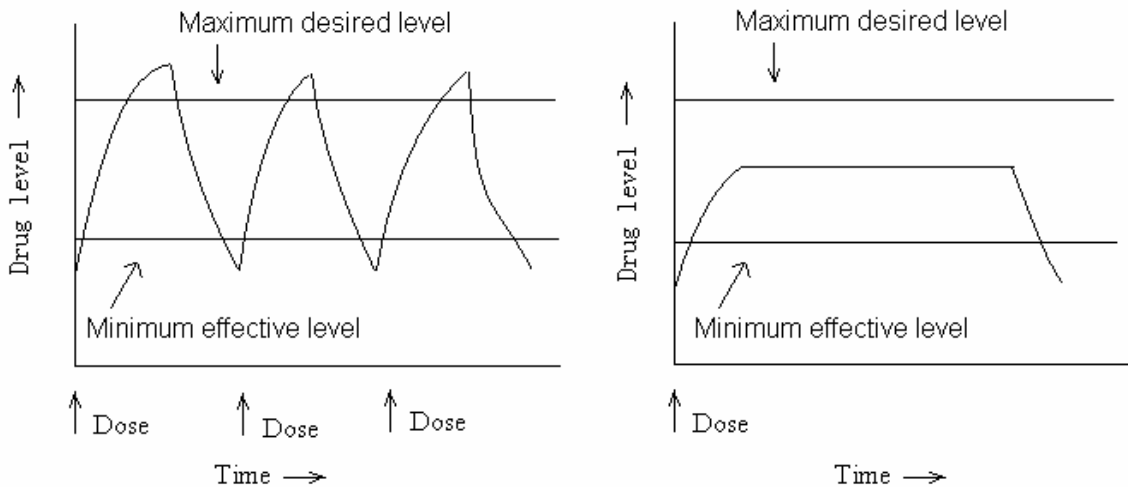


Fig 5 Drug levels in the blood with (Left) traditional drug dosing and (Right) controlled delivery dosing

2.2 BRAIN CANCER AND OTHER BRAIN DISEASES

A brain tumor is a mass of unnecessary cells growing in the brain [94]. There are two basic kinds of brain tumors: primary brain tumors and metastatic brain tumors [95]. Primary brain tumors start, and tend to stay, in the brain. Metastatic brain tumors begin as cancer elsewhere in the body and spread to the brain. Primary brain tumors occur in people of all ages, but they are statistically more frequent in two age groups, children under the age of 15 and older adults. Metastatic brain tumors are much more common in adults. An estimated 40,900 new cases of primary brain tumors are expected to be diagnosed in 2004. This is based on an incidence rate of 14 per 100,000 persons and a projected 2004 U.S. population of 285,266,000. The incidence statistics stated above include those with all primary brain tumors, both malignant and benign, and are based on the year 2004 population. In the United States, approximately 3,140 children younger than age 20 are diagnosed annually with primary brain tumors. Brain tumors are the most common of the solid tumors in children, and the second most frequent malignancy of childhood. Although statistics for brain metastases are not readily available, it is estimated that over 100,000 cancer patients per year will have symptoms due to metastatic brain tumors and up to 80,000 per year will have a metastatic tumor in the spinal cord [96].

Surgery is the chief form of treatment for brain tumors that lie within the membranes covering the brain or in parts of the brain that can be removed without damaging critical neurological functions [97]. Because a tumor will recur if any tumor cells are left behind, the surgeon's goal is to remove the entire tumor whenever possible.

Radiation therapy and chemotherapy, in general, are used as secondary or adjuvant treatment for tumors that cannot be cured by surgery alone. Chemotherapy works to destroy tumor cells with drugs that may be given either alone or in combination with other treatments [97].

2.3 NANOPARTICLE TECHNOLOGY

2.3.1 Introduction of Nanoparticles

Nanoparticles are solid colloidal particles ranging in size from 10 to 1000 nm. Nanoparticles can serve as a novel drug delivery carriers to tissues throughout the body. This is accomplished by masking the membrane barrier, limiting characteristics of the therapeutic drug molecules, as well as retaining drug stability, with that of the properties of the colloidal drug carrier. Once the nanoparticles reach the desired tissue, release of the drug may occur by desorption, diffusion through the nanoparticles matrix or polymer wall or nanoparticles erosion, or some combination of any or all mechanisms.

The nanometer size-ranges of the drug delivery systems offer certain distinct advantages for drug delivery due to their sub-cellular and sub-micron size, nanoparticles can penetrate deep into tissues through fine capillaries, cross the generation present in the epithelial lining, and are generally taken up efficiently by the cells [98]. Nanoparticles have in general relatively high intracellular uptake compared to microparticles. Previous studies show that particle size significantly

affects cellular and tissue uptake, and in some cell lines, only the submicron size particles are taken up efficiently but not the larger size microparticles [99]

2.3.2 Fabrication Techniques of Nanoparticles

Nanoparticles can be fabricated in different ways according to the polymers used and the properties of the drugs. Generally, they can be divided into two categories, dispersion of preformed polymers and polymerization methods.

2.3.2.1 Dispersion of preformed polymers

Solvent evaporation method [100]

In this method, the polymer is dissolved in an organic solvent. The drug is dissolved or dispersed into the preformed polymer solution, and this mixture is then emulsified into an aqueous solution to make an oil (O) in water (W) emulsion by using a surfactant/emulsifying agent like poly (vinyl alcohol), polysorbate-80, poloxamer-188, etc. After the formation of a stable emulsion, the organic solvent is evaporated by increasing the temperature/under pressure or by continuous stirring.

Spontaneous emulsification/ solvent diffusion method [101]

This method is a modified version of the solvent evaporation method. Briefly, the water-soluble solvent along with the water insoluble organic solvent was used as an oil phase. Due to the spontaneous diffusion of water-soluble solvent, an interfacial turbulence is created between two phases leading to the formation of smaller particles.

As the concentration of water-soluble solvent (acetone) increases, a considerable decrease in particle size can be achieved.

Salting out/ emulsification-diffusion method

Salting-Out [102]

In this method, polymer and drug are dissolved in acetone. The solution is then emulsified under vigorous mechanical stirring in an aqueous gel containing the salting-out agent and a colloidal stabilizer. This oil-in-water emulsion is diluted with a sufficient volume of water or aqueous solutions to enhance the diffusion of acetone into the aqueous phase, thus inducing the formation of nanoparticles. The remaining solvent and salting-out agent are eliminated by cross-flow filtration.

Emulsification-Diffusion [103]

This method can be considered as a modification of the salting-out procedure, avoiding the use of salts and hence intensive purification steps. It involves the use of a partially water-soluble solvent, which is previously saturated in water to ensure the initial thermodynamic equilibrium of both liquids. The polymer is dissolved in the water-saturated solvent, and this organic phase is emulsified, under vigorous agitation, in an aqueous solution containing a stabilizer. The subsequent addition of water to the system causes the solvent to diffuse into the external phase, resulting in the formation of nanoparticles.

Supercritical fluid technology [104]

In the rapid expansion of supercritical solution (RESS) method the solute of interest is solubilized in a supercritical fluid and the solution is expanded through a nozzle. Thus, the solvent power of supercritical fluid dramatically decreases and the solute eventually precipitates.

2.3.2.2 Polymerization methods

Emulsion polymerization [105]

Emulsion polymerization characterizes both radical and anionic polymerization. The process consists of building a chain of polymers, which acts as the drug carrier, from single monomer units of a given compound. Polymerization occurs spontaneously at room temperature after initiation by either free radical or ion formation. Triggers for polymer growth include high-energy radiation, UV light, or hydroxyl ions. Once polymerization is complete, the solution is filtered and neutralized to remove any residual monomers. The polymers form micelles and droplets (nanoparticles), consisting of approximately 100 to 10^7 polymer molecules. The mass of polymers inherent in this type of nanoparticle formulation provides the available space that acts as a carrier for adsorption or absorption of the drug.

Emulsion polymerization can also be accomplished in an organic phase rather than an aqueous phase. This process has been adapted for use with polyalkyl-cyanoacrylate nanoparticles.

Interfacial polymerization [106]

Interfacial polymerization is similar to emulsion polymerization in that monomers are used to create polymers. However, the mechanism is different. Interfacial polymerization occurs when an aqueous and organic phase are brought together by homogenization, emulsification, or micro-fluidization under high-torque mechanical stirring. This precludes the inclusion of peptide/proteins at this step secondary to mechanical shearing.

A subset of interfacial polymerization is the process of adding a solvent mixture of benzyl benzoate, acetone, and phospholipids to the organic phase containing the drug and monomer. It has been suggested that this process encourages the formation of the nanocapsule shell between the aqueous phase and the benzyl benzoate drops in the organic phase. One advantage of interfacial polymerization may be the encapsulation of the drug. Once the drug is encapsulated, it is protected until it reaches the target tissue and degradation occurs. In the case of CNS delivery, it is desirable to protect or disguise the drug until it is past the barrier and can be released into the brain.

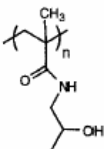
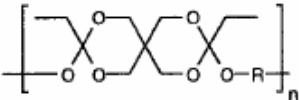
2.4 BIODEGRADABLE POLYMERS FOR CONTROLLED DRUG DELIVERY

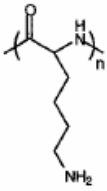
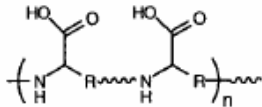
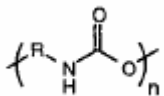
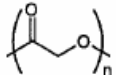
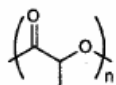
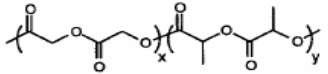
2.4.1 Biodegradable Polymers in Drug Delivery Systems

Biodegradable polymers are widely used in controlled drug delivery systems because they can be expelled by human body and cause no harm to human. The biodegradable polymers in drug delivery can be divided into two categories: natural biodegradable

polymers and synthetic biodegradable polymers. Natural biodegradable polymers like bovine serum albumin (BSA), human serum albumin (HSA), collagen, gelatin, hemoglobin have been studied. However, the use of them is limited due to their higher costs and questionable purity. Since last two decades, synthetic biodegradable polymers have been increasingly used to deliver drugs, since they are free from most of the problems associated with the natural polymers. Poly (amides), poly (amino acids), poly (alkyl- α -cyano acrylates), poly (esters), poly (orthoesters), poly (urethanes), and poly (acrylamides) have been used to prepare various drug loaded devices. Table 1 below show the structures of some biodegradable polymers mentioned here.

Table 2 Structures of biodegradable polymers usually used in drug delivery

Polymer	Notes
Poly(acrylamides) e.g., poly(N-(2-hydroxypropyl) methacrylamide) <div style="text-align: center;">  </div>	Plasma expander used as polymer-drug conjugate for distribution control. [107] Enzyme cleavable side chains employed to target release at colon [108]. Hydrolytically degradable hydrogels produced by crosslinking with N, O-dimethacryloyl hydroxylamine linker [109]. Component of photosensitive delivery system [110].
Poly(ortho esters) e.g., 3,9-diethylidene 2,4,8,10-tetraoxaspiro[5.5]undecane-based polymers <div style="text-align: center;">  </div>	inhibit drug release by diffusion mechanisms and allow drug release only after the hydrolysis of the polymer chains at the surface of the device [111]

<p>Poly(amino acids) e.g., poly(lysine)</p>  <p>pseudo-poly(amino acids)</p> 	<p>Poly(lactic acid-co-lysine) (PLAL)</p>
<p>Poly(urethanes)</p> 	<p>Hard and soft segment polymers containing PEG for temporal controlled release [112, 113].</p> <p>Azo-containing polymers used to control site of polymer-drug conjugate degradation [114].</p> <p>Anti-infectious biomaterials containing antibiotics [115].</p>
<p>Poly(glycolic acid) (PGA)</p>  <p>Poly(lactic acid) (PLA)</p> 	<p>copolymer: Poly(lactic acid-co-glycolic acid) (PLGA)</p>  <p>Biosynthetic poly(ester) often employed as copolymer with hydroxyvalerate monomer.</p>

Among the biodegradable polymers, the thermoplastic aliphatic poly (esters) like PLA, PGA and especially their copolymer PLGA have generated tremendous interest

due to their excellent biocompatibility and biodegradability. They are widely used in the nanoparticulate drug delivery systems.

2.4.2 Poly (lactide-co-glycolide) (PLGA)

Poly (lactide-co-glycolide) (PLGA) is the best characterized and most widely studied biodegradable polymer. Moreover, it is a FDA approved material. It is especially widely used in the form of microspheres and nanoparticles as controlled drug delivery systems.

PLGA is the copolymer of PLA and PGA. The structure of these two polymers can be found in table 3. They are both poly (ester). The polymer PLA can exist in an optically active stereoregular form (L-PLA) and in an optically inactive racemic form (D, L-PLA). L-PLA is found to be semicrystalline in nature due to high regularity of its polymer chain while D, L-PLA is an amorphous polymer because of irregularities in its polymer chain structure. Hence, D, L-PLA is more used than L-PLA since it enables more homogeneous dispersion of the drug in the polymer matrix. PGA is highly crystalline because it lacks the methyl side groups of the PLA. Lactic acid is more hydrophobic than glycolic acid. Thus lactide-rich PLGA copolymers are less hydrophilic, absorb less water, and degrade more slowly.

By varying the monomer ratios in the polymer processing and by varying the processing conditions, the resulting polymer can exhibit drug release capabilities for months or even years.

Both, in vitro and in vivo the PLGA copolymer undergoes degradation in an aqueous environment (hydrolytic degradation or biodegradation) through cleavage of its backbone ester linkages. The polymer chains undergo bulk degradation and the degradation occurs at uniform rate throughout the PLGA matrix. It has been reported that the PLGA biodegradation occurs through random hydrolytic chain scissions of the swollen polymer. The carboxylic end groups present in the PLGA chains increase in number during the biodegradation process as the individual polymer chains are cleaved; these are known to catalyze the biodegradation process. The biodegradation rate of the PLGA copolymers are dependent on the molar ratio of the lactic and glycolic acids in the polymer chain, molecular weight of the polymer, the degree of the crystallinity, and the Tg of the polymer [116].

The PLGA polymer degrades into lactic and glycolic acids. Lactic acid enters the tricarboxylic acid cycle and is metabolized and subsequently eliminated from the body as carbon dioxide and water. In a study conducted using ¹⁴C-labeled PLA implant, it was concluded that lactic acid is eliminated through respiration as carbon dioxide. Glycolic acid is either excreted unchanged in the kidney or it enters the tricarboxylic acid cycle and eventually eliminated as carbon dioxide and water.

The drug entrapped in PLGA matrix is released at a sustained rate through diffusion of the drug in the polymer matrix and by degradation of the polymer matrix.

2.4.3 Poly (Lactic acid) – poly (ethylene glycol) (PLA-PEG) Copolymers

PLA-PEG copolymers and their use as an effective biomaterial in drug delivery and tissue engineering have been well characterized [117-123]. PLA is the backbone of the polymer. Polyethylene glycol (PEG) is widely used to cloak the particles and obtain stealthy properties. With one end being adsorbed on or attached to the particles surface, PEG chain extrudes outwards to form hydrophilic and flexible “conformational clouds”, which become an effective protective layer to inhibit the opsonization [124-127].

2.5 NANOPARTICLES OF BIODEGRADABLE POLYMERS TO PENETRATE THE BLOOD BRAIN BARRIER

2.5.1 Ideal Properties of Nanoparticles across the Blood Brain Barrier

There have been intensive investigations focused on nanoparticles for drug delivery across the BBB. Jorg Kreuter is the first one who successfully developed polysorbate-coated polybutylcyanoacrylate nanoparticles to deliver an analgesic drug dalargin into the brain [63]. Maltodextrin [128], stearic acid [129], and Emulsifying Wax & Brij 78 [130] particles had also been investigated for drug delivery across the blood brain barrier.

As mentioned in the methods to penetrate the blood brain barrier, nanoparticles of biodegradable polymers may be a promising strategy to overcome the blood brain barrier. In P.R. Lockman’s paper [20], the ideal properties of nanoparticle based drug delivery system for drug delivery across the blood brain barrier were discussed. Table 3 shows a list of ideal propertis of polymeric-based nanoparticles for drug delivery to

cross the blood brain barrier. However, these are only general ideal properties for the nanoparticles. When the particles are used for a certain drug or agent, the properties of the drug or agent must also be considered as the encapsulation efficiency of the nanoparticles to the drug are also very important, especially for some expensive drugs.

Table 3 *Ideal properties of polymeric-based nanoparticles for drug delivery across the BBB [20]*

Natural or synthetic polymer
Inexpensive
Nontoxic
Biodegradable/ biocompatible
Nonthrombogenic
Nonimmunogenic
Particle Diameter < 100nm
Stable in blood (i.e., no opsonization by proteins)
BBB-targeted (i.e., use of cell surface ligands, receptor-mediated endocytosis)
No activation of neutrophils
No platelet aggregation
Avoidance of the reticuloendothelial system
Noninflammatory
Prolonged circulation time
Scalable and cost-effective with regard to manufacturing process
Amenable to small molecules, peptides, proteins, or nucleic acids

2.5.2 Possible Mechanism of Nanoparticles to Penetrate the Blood Brain Barrier

To date, the exact transport mechanisms of nanoparticle across the BBB are not fully understood. Kreuter and colleagues proposed the following possible mechanisms for

nanoparticle mediated drug uptake by the brain which could contribute alone or in combination [63]:

1. Enhanced retention of nanoparticles in the brain blood capillaries with an adsorption to the capillary wall. This leads to the creation of a high concentration gradient that enhances transport across the BBB.
2. Surfactant effect produced by the polysorbate coating resulted in the solubilisation of endothelial cell membrane lipids and membrane fluidization, thus enhanced the penetration of drug through the BBB.
3. The presence of nanoparticles leads to an opening of the tight junction between the endothelial cells. The drug could permeate through in free form or together with the nanoparticles in bound form.
4. Polysorbate 80 coating facilitates nanoparticles interaction with the BBB endothelial cells, leading to endocytosis of nanoparticles followed by the release of the drug within these cells and delivery to the brain.
5. Nanoparticles with bound drug could be transcytosed through the endothelial cell layer.
6. Polysorbate 80, as the coating agent, could inhibit the efflux system, especially P-gp.

The mechanism of the nanoparticle-mediated transport of the drugs across the blood-brain barrier at present is not fully understood yet. Several possible routes have been summarized which include paracellular pathway, transcellular pathway, transport, specific endocytosis and adsorptive endocytosis. Considering the property of the

nanoparticles, it is easy to find that the possibility of the first three pathways is very low. The most likely mechanism for nanoparticles to cross the blood brain barrier is endocytosis by the endothelial cells lining the brain blood capillaries.

As seen in Kreuter's publications [62], nanoparticle-mediated drug transport to the brain depends on the over-coating of the particles with polysorbates, especially polysorbate 80. It was proposed that over-coating with these materials seems to lead to the adsorption of apolipoprotein E from blood plasma onto the nanoparticle surface. The particles then seem to mimic low density lipoprotein particles and could interact with the LDL receptor leading to their uptake by the endothelial cells. After this the drug may be released in these cells and diffuse into the brain interior or the particles may be transcytosed. Other processes such as tight junction modulation or P-glycoprotein inhibition also may occur. These mechanisms may run in parallel or may be cooperative thus enabling a drug delivery to the brain. From the possible mechanism of nanoparticles to penetrate the blood brain barrier, it can be seen that surface modification of the nanoparticles may be very important.

2.5.3 Surface Modification of Nanoparticles

To penetrate the blood-brain barrier, the surface properties of the nanoparticles are very important. It is because the hydrophobicity is one of the important factors that determine the passive diffusion of substances across the brain endothelial cells. Furthermore, as mentioned in the previous part, surface coating of the nanoparticles may lead to specific endocytosis.

In J. Kreuter et. al. 's study, the ability of 12 different surfactants, (Polysorbate 20, 40, 60, 80, Polyoxyethylene-(23)-laurylether (Brij® 35), Poloxamers 184, 188, 338, 407, Poloxamine 908, Cremophor® EZ, RH 40), coated onto the surface of nanoparticles, to facilitate the delivery of a nanoparticles-bound model drug, dalargin, was investigated [62]. The leu-enkephalin analogue hexapeptide dalargin was bound to polybutylcyanoacrylate nanoparticles by sorption for 3 h. Different surfactant were then coated over these nanoparticles and were injected intravenously into mice. Nociceptive analgesia was then measured by the tail-flick test 15, 30, 45 and 90 min after injection. Only nanoparticles that had been boated with polysorbate 20, 40, 60 and 80 yielded a significant effect. The highest effect was observed with polysorbate. Maximum effects were found after 15 min, at a dalargin dosage of 10 mg/kg, and after 45 min, with 7.5 mg/kg.

2.6 MRI AND MRI CONTRAST MEDIUM

MR imaging is a imaging method using a strong magnetic field and gradient fields to localize bursts of radiofrequency signals coming from a system of spins consisting of reorienting hydrogen H nuclei after they have been disturbed by radiofrequency RF pulses. MR imaging produces high resolution, high contrast two-dimensional image slices of arbitrary orientation, but it is also a true volume imaging technique and three-dimensional volumes can be measured directly. Applications of MR imaging have steadily widened over the last decade. Currently it is the preferred cross-sectional imaging modality in most diseases of the brain and spine and has attained major importance in imaging diseases of the musculoskeletal system. MR imaging in

the head and neck and pelvis has attained a substantial level of clinical use, and its applications in the abdomen, kidneys and chest are rapidly increasing with the advent of ultrafast MR imaging techniques.

Contrast medium is various agents used to facilitate distinction between structures on images as a consequence of differences in contrast. MR contrast media either act predominantly on T1 relaxation which results in signal enhancement and "positive" contrast, or on T2 relaxation, which results in signal reduction and "negative" contrast.

The positive contrast agents are typically small molecular weight compounds containing as their active element Gadolinium Gd , Manganese Mn or Iron Fe , all of which have unpaired electron spins in their outer shells and long relaxivities which make them good T1 relaxation agents

Diethylenetriaminepentaacetic acid gadolinium(III) dihydrogen salt hydrate (Gd-DTPA) ($C_{14}H_{20}GdN_3O_{10} \cdot xH_2O$ 547.57) is widely used metal ion complex for MRI used in the diagnosis of cerebral tumors, CNS diseases, hepatic tumors, pituitary adenomas, multiple sclerosis, and blood-brain barrier impairment.

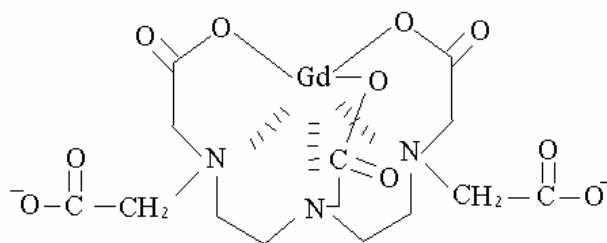


Fig. 6 Chemical structure of Gd-DTPA

CHAPTER THREE

MATERIALS AND METHODS

3.1 MATERIALS

Poly (D,L-lactide-co-glycolide) (PLGA, 50:50, MW 40000-75000), polyvinyl alcohol (PVA MW 30000-70000), were purchased from Sigma chemical Co. USA. Paclitaxel was purchased from Dabur India Limited, India and Hande Biotechnology Inc., China. Tween 80 was purchased from ICN biomedical company. Vitamin E succinate with polyethylene glycol 1000 (Vitamin E TPGS) was provided by Eastman Chemical Company (USA). F68 and F127 were provided by BASF. Cormarin -6 was purchased from Aldrich Chem. Co. The solvent dichloromethane (DCM, analytical grade) was purchased from Mallinckrodt. Acetonitrile for HPLC/ Spectro use (FW=41.05) was purchased from Tedia. Madin-Darby canine kidney (MDCK) epithelial cell line was phased from American Type Culture Collection (CCL-34) and passages 58-70 were used. Hank's balanced salt solution (HBSS), Penicillin Streptomycin, Dulbecco's Modification of Eagle's Medium (DMEM), and PBS were purchased from sigma. Fetal calf serum was purchased from Hyclone. Fm4-64 was phased from molecular probes. Triton 100 was purchased from BDH limited Poole England. Deionized water produced by Millipore (Millipore Corporation, Bedford, MX 01730, USA) was used throughout. Gadolinium-DTPA was purchased from Sigma. PLA-PEG was provided by Dong Yuancai.

3.2 METHODS

3.2.1 *In Vitro* Evaluation of PLGA Nanoparticles for Paclitaxel Delivery Across the Blood Brain Barrier

3.2.1.1 Fabrication of nanoparticles

PLGA nanoparticles were prepared by the single emulsion solvent evaporation method. Briefly, 110 mg PLGA and 5.5 mg paclitaxel were dissolved in 8 ml DCM to form the organic phase. The organic phase was poured slowly into 120 ml water with 0.6g PVA or 36mg VE-TPGS. The mixture was then sonicated for 120 seconds and the resultant emulsion was stirred overnight with a magnetic stirrer to allow for the evaporation of the organic solvent. The nanoparticles were collected by centrifugation at 11200 rpm for 15 min. Then the particles were washed with distilled water for three times by centrifugation to remove the excess emulsifier. The naked nanoparticles were then incubated in the solutions of 0.5% (w/v) coating materials for three hours and washed by centrifugation for three times again. Finally, the products were freeze dried to obtain fine powders, which was kept in vacuum desiccator for future use.

The fluorescence nanoparticles were prepared using the same method while cormorin-6 was used as a fluorescence marker instead of paclitaxel.

3.2.1.2 Nanoparticles characterizations

Size and size distribution

The particle size and size distribution of the nanoparticles were measured by the laser light scattering (Brookhaven Instruments Corporation 90 plus Particle Sizer) at 25°C and at a scattering angle of 90°. The dried nanoparticles were suspended in deionised water by sonication and determined for the volume mean diameter, size distribution and polydispersity.

Zeta potential

Zeta potential was measured by the laser Doppler anemometry (Zeta Plus, Zeta potential Analyzer, Brookhaven Instruments Corporation). The particle was re-suspended in deionized water before measurement. The value was recorded as the average of five measurements.

Morphology

Scanning electrical microscopy (SEM) and atomic force microscopy (AFM) were employed to determine the shape and surface morphology of the nanoparticles. Before SEM observation, the particles were fixed on a tip and coated with platinum by an Auto Fine Coater (JFC-1300, JEOL USA). AFM was conducted with Nanoscope IIIa in the tapping mode. The nanoparticle sample was mounted on a metal slabs using double-sided adhesive tapes and scanned by the AFM maintained in a constant-temperature and vibration-free environment.

3.2.1.3 Encapsulation efficiency of paclitaxel

This experiment was performed in triplicates using high performance liquid chromatography (HPLC) to determine the concentration of paclitaxel extracted from the nanoparticles. Briefly, 3 mg of nanoparticles was dissolved in 1 ml of DCM to extract paclitaxel from the nanoparticles. DCM was allowed to evaporate overnight. 3 ml of acetonitrile/ water (50:50, v/v) was added and the solution was vortexed for 1 min. After which, the sample was filtered through a filter membrane (0.45 μ m pore size) and transferred to HPLC vials. The mobile phase of HPLC was composed of acetonitrile and water of 50/50 (v/v).

3.2.1.4 *In vitro* release of paclitaxel

The release of paclitaxel from the nanoparticles was measured using HPLC. Five batches of particles that were made were used for the study. The study was carried out in triplicates. 5 mg of the paclitaxel-loaded nanoparticles were weighed into individual centrifuge tubes and suspended in 10 ml of fresh PBS. The tubes were placed in a 37°C orbital shaker water bath and shaken horizontally at 120 min⁻¹.

The tubes were taken out at particular time intervals and centrifuged at 13000, 18°C, 15 minutes. The supernatant was removed and taken for *in vitro* release analysis.

The precipitated nanoparticles were re-suspended in 10 ml PBS, sonicated, vortexed and placed back into the water bath shaker. Paclitaxel in the supernatant was extracted in 1 ml of DCM in a separation funnel. The funnel was shaken consistently and 2 layers would form. The top layer contained water while the bottom layer contained DCM and the extracted paclitaxel. DCM was collected and allowed to

evaporate overnight. 3 ml of acetonitrile/ water was added after evaporation and 1ml of the solution was transferred to the HPLC vials. The condition of the HPLC analysis was the same as described in the determination of encapsulation efficiency.

3.2.1.5 Cell culture and cellular uptake experiments

Cell culture

MDCK cells were cultured in 25 ml flasks in a humidified 5% CO₂/95% air incubator at 37°C. The culture medium was DMEM supplemented with 10% FBS, 100 ug/ml penicillin G and 100 ug/ml streptomycin sulfate. After growing to confluent, the cells were washed with 5 ml PBS and rinsed with 2 ml trypsin twice. Then, 3 ml trypsin was added to the cells and the flask was kept in the incubator at 37°C for about 15 minutes. Five ml medium were added to the flask and the cell suspension were transferred to a 15 ml centrifuge tube. The cells were collected by centrifugation for 5 minutes at 1000 rpm.

Cellular uptake experiments

For quantitative uptake experiments, MDCK cells were seeded in 96 well plates. After the cells reached confluent, the medium was removed and replaced with 100 ul of Hank's balance salt solution (HBSS). Cells were incubated for 1 h in HBSS for balance. Fluorescence labeled nanoparticles suspensions of different concentrations were then added to the cells and the plate was incubated for 4 hours. Uptake was terminated by washing the cells for three times using PBS. The cells were solubilized by triton/0.2N NaOH. The plate was then scanned with a micro plate reader

(excitation wavelength 430 nm, emission wavelength 485 nm) to measure the amount of fluorescence in each well.

For confocal laser scanning microscopy imaging, MDCK cells were seeded at a low density in 4-chamber coverless system and were observed next day after seeding. The medium was removed and replaced with 500 ul of HBSS. Cells were incubated for 1 h in HBSS and fluorescence labeled nanoparticles suspensions were added to the cells. After 1 hour incubation, nanoparticles suspensions were removed and the cells were washed with PBS for three times. The cells were then fixed with formaldehyde and the cell membrane was counterstained with fm4-64 for 1 hour at the room temperature. Then the cells were observed under confocal laser scanning microscopy.

3.2.2 Gd-DTPA Loaded Nanoparticles of Biodegradable Polymers for MRI of the Brain

3.2.2.1 Fabrication of nanoparticles

To prepare Gd-DTPA loaded nanoparticles, three polymers were used, including PLGA, PLA-PEG (90:10), and PLA-PEG (70:30). PLA-PEG copolymers were synthesized by Mr Dong Yuancai in the Chemotherapeutic Engineering laboratory of NUS. The nanoprecipitation method was used to prepare Gd-loaded nanoparticles. Briefly, 75mg polymer was dissolved in certain amount of acetone, and 0.3ml Gd-DTPA solution was suspended in the polymer solution by sonicated by 20 seconds. The resultant suspension was added drop by drop to 25ml water with 100 mg F-68. The organic solvent was then evaporated under vacuum. Finally, the particles were

collected by centrifugation at 12,000 rpm for 80 minutes and freeze dried to obtain fine powder.

3.2.2.2 Encapsulation efficiency of Gd-DTPA

The encapsulation efficiency and drug content of the particles were studied by inductively coupled plasma-atomic emission spectrometry (ICP-AES). Briefly, certain amount of particles was dissolved by 1 ml DCM and vortexed for 3 minutes. After that, DCM was evaporated. Gd-DTPA was extracted by water. Then the samples were filtered by 0.22µm syringe driven filters and the concentration of Gd in the solution was determined by ICP-AES.

3.2.2.3 *In vitro* release of gadolinium

The *in vitro* release profile of gadolinium from the particles was studied in PBS at 37°C and the method was based on a dynamic dialysis. The study was carried out in triplicates. Briefly, the Gd-DTPA loaded nanoparticles were dispersed using 5 ml PBS inside dialytic tubing and were incubated in 35 ml of extra-dialytic tubing PBS with shaking. Sampling was carried out at predetermined time intervals from extra-dialytic tubing test medium. The same amount of PBS was added to the extra-dialytic medium. Released gadolinium in the sample was measured by ICP-AES.

3.2.2.4 *In vitro* and *in vivo* MRI

Before the Gd-DTPA loaded nanoparticles were used on animals, *in vitro* test in tube was carried out. Briefly, the particles were suspended in water and scanned by MRI

first. Then, the suspension was filtered by a 220 nm syringe driven filter. The filtration was scanned by the MRI. The values indicating the density of gadolinium before and after filtering were compared to find out the amount of released and remaining gadolinium in the particles.

For in vivo MRI experiment, healthy rats about 200-220 g were used. Each rat was intravenously injected at a dose of 1 ml in tail vein, respectively. Those injections were suspensions containing the preparations of nanoparticles. The animals were scarified 1 hour after injection. The animals were then scanned by MRI.

CHAPTER FOUR

RESULTS AND DISCUSSION

4.1 *IN VITRO* EVALUATION OF PLGA NANOPARTICLES FOR PACLITAXEL DELIVERY ACROSS THE BLOOD BRAIN BARRIER

4.1.1 Particle Size and Size Distribution

Totally five batches of PLGA nanoparticles were prepared by the method of single emulsion solvent evaporation. Sample 1 was PLGA nanoparticles emulsified with PVA. Sample 2, 3 and 4 were the PVA emulsified PLGA nanoparticles coated with Tween 80, poloxamer 188 and poloxamer 407, respectively. Sample 5 was VE-TPGS emulsified PLGA nanoparticles. The size averaged by particle volume and polydispersity of all samples were determined by laser light scattering. Table 4 shows the particle size and size distribution of the particles. The results are mean value of 6 measures.

Particle size plays important roles in determining the intracellular uptake of nanoparticles and determining the fate of the nanoparticles after administration. It is also one of the key factors in determining whether the particle can cross the blood brain barrier. It was reported that smaller particles tended to accumulate in the tumor site due to the facilitated extravasation [131] and a greater internalization was also observed [132]. Particles less than 200 nm can prevent spleen filtering [133]. In

addition, smaller particles make intravenous injection easier and their sterilization may be simply done by filtration [134, 135].

In our study, as shown in table 4 below, the size of all the particles was within 250 to 280 nm. A variety of particles ranged in size from less than 100 nm to more than 300 nm had been investigated to cross the blood brain barrier [136-139]. Generally particles in size from 250 to 280 were possible to cross the blood brain barrier. For Sample 1, the PVA emulsified nanoparticles, had a size of 257.1 nm. When the particles were coated with tween 80, poloxamer 188 and poloxamer 407, the sizes were increased by 1.5, 27.0, and 11.1 nm, respectively. The increase of the sizes could be attributed to the formation of an adsorbed coating layer on the particle surface. All the three coating materials are amphiphilic molecules and they may be adsorbed to the particle surfaces from an aqueous solution through hydrophobic interaction of the hydrophobic moiety with the particle surface. The hydrophilic blocks extend into the aqueous medium to form a hydrophilic layer. The thickness of the layer may be determined by the length of the hydrophilic part of the molecule and the conformation of the hydrophilic part. This may explain the different on size increase of the coated particles. For sample 5, the particles emulsified with VE-TPGS, the size was 14 nm larger than that of sample 1. It may due to the structure of the emulsifiers. As shown in figure below, the structure of PVA is a long linear chain. The molecular weight is 30000-70000. VE-TPGS is a water-soluble derivative of natural vitamin E, which is formed by esterification of vitamin E succinate with polyethylene glycol 1000. The molecular weight of VE-TPGS is only 1,513, which is much lower than that of PVA. In the formation of the nanoparticles, the emulsifier

was on the interface of oil droplet and the water phase, and helped to stabilize the nanoemulsion droplet. The long chain of PVA made it more effective in stabilizing the droplet which led to smaller particles. However, considering the amount of PVA (0.6g) and VE-TPGS (36mg) used, the emulsifying efficiency of TPGS was much bigger than that of PVA. This could be due to the unique physicochemical properties of Vitamin E TPGS. VE-TPGS is miscible with water and forms a solution with water at a concentration up to ~20% (w/w), beyond which liquid crystalline phases may form. The amphiphilic characteristic of the TPGS molecule leads to its self-association in water when the concentration exceeds a threshold known as the critical micelle concentration (CMC), which is ~0.02 wt% in water. Above CMC, TPGS begins to form micelles and continues to form relatively low viscosity solutions with water until a concentration of ~20 wt% is obtained. When the TPGS concentration is above this value, higher viscosity liquid crystalline phases start to form. In the fabrication of nanoparticles by the single emulsion solvent evaporation technique, the role of the surfactant stabilizer is to stabilize the dispersed-phase droplets and inhibit coalescence. The amphiphilic surfactants align themselves at the droplet surface so as to promote stability by lowering the free energy at the interface between two phases and resisting coalescence and flocculation of the nanoparticles. However, at higher concentrations, the state of TPGS in the aqueous dispersing phase has changed and it can no longer exert a stabilizing effect on the formation of the emulsion system, droplet separation and stabilization, as well as nanoparticle hardening. In contrast, it was evident that when the concentration was too low, it did not act as an emulsifier. Therefore, TPGS would not be able to perform as a good surfactant at both higher and

lower concentrations and could not produce nanoparticles with ideal properties. This may be explained that TPGS at low concentration was a good emulsifier for PLGA nanoparticle fabrication. This characteristic of VE-TPGS makes it a good emulsifier because the low amount used in nanoparticle preparation leads to easy washing of the remaining emulsifier on the surface of the particles. Moreover, VE-TPGS may have the potential to improve nanoparticle adhesion to cells and the hemodynamic properties of the nanoparticles in the blood flow while remaining PVA has negative effects on cellular uptake of the particles. This provides advantages of VE-TPGS emulsified nanoparticles to the PVA emulsified particles. From table 4 it can also be seen that the polydispersity of the particles was from 0.009 to 0.17. The relatively low polydispersity indicated that the particles prepared by single emulsion solvent evaporation method had a narrow distribution of the particle size.

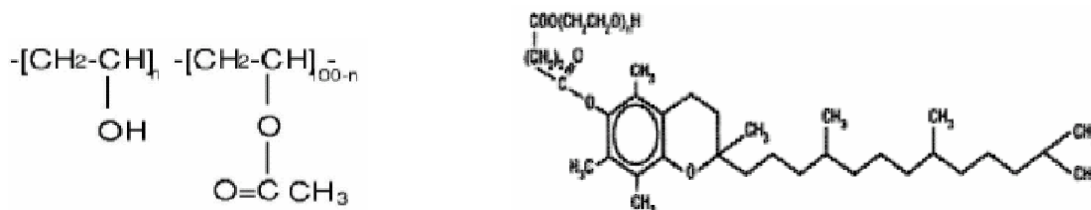


Fig 7 Chemical structure of PVA and VE-TPGS

Sample	Matrix/Emulsifier/Coating	Particle Size (nm)	Polydispersity
1	PLGA /PVA/--	257.1	0.113
2	PLGA /PVA/Tween 80	257.6	0.126
3	PLGA /PVA/Poloxamer 188	284.1	0.009
4	PLGA /PVA/Poloxamer 407	268.0	0.101
5	PLGA /TPGS/--	274.1	0.17

Table 4: Size and Size Distribution of different nanoparticles

4.1.2 Zeta Potential

Zeta-potential indicates the surface charge of the nanoparticle. The surface charge can greatly influence the particles stability in suspension through the electrostatic repulsion between the particles. It is also an important factor to determine their interaction in vivo with the cell membrane, which is usually negatively charged. In addition, from the surface charge the dominated component on the particle surface can be roughly known.

The zeta potential of the five samples was measured by the laser Doppler anemometry. The results are shown in table below. The results were mean value of 6 measures. From the results it can be seen that the zeta potential of all the five samples was negative. The zeta potential of sample 1, the PVA emulsified nanoparticle was -13.72 mV. When the particles were coated with Tween80, poloxamer 188 and poloxamer 407, the particles tended to be more negatively charged. For sample 5, the particles emulsified with VE-TPGS, they were even more negatively charged than all the PVA emulsified particles.

Generally, the surface charge of the nanoparticles was determined by the materials presented on the surface of the nanoparticles. In our study, the particles were prepared using PLGA, PVA or TPGS and the surface coating materials. It has been reported that the zeta potential of PLGA nanoparticles without any PVA in neutral buffer is about -45 mV [140]. This high negative charge is attributed to the presence of uncapped end carboxyl groups of the polymer at the particle surface. But the zeta potential of our nanoparticles could not be -45 mV because there were remaining

emulsifiers or coating materials on the surface of the particles. In several studies, a clear differentiation in the zeta potential values of coated and non-coated nanoparticles was reported, with generally highly negative zeta potential values for non-coated nanoparticle and less negative zeta potential values for coated nanoparticles. Coating of nanoparticles with some amphiphilic polymers normally decreases the zeta-potential because the coating layers shield the surface charge and move the shear plane outwards from the particle surface [141, 142]. Redhead et al. have reported a similar reduction in the zeta potential of PLGA nanoparticles after coating with amphiphilic polymers like poloxamer 407 and poloxamine 908 [143]. In our study, the first four samples were emulsified by PVA. PVA on the particle surface could not be moved completely even after repeated washings because it forms an interconnected network with the PLGA at the interface. The remaining PVA may shield the surface charge of PLGA. This may explain why the zeta potential of sample 1 was -13.72 mV. Sample 2, 3, 4 were coated with Tween 80, poloxamer 188 and poloxamer 407, respectively. The zeta-potential results reflected the presence of the adsorbed layer on the particle surface. A reduction of the absolute value of the zeta potential indicated that the particles were successfully coated with these materials in the solution. For sample 5, the VE-TPGS emulsified nanoparticles, it had a zeta potential which was more negative than all the other samples. Compared with sample 1, the PVA emulsified nanoparticles, the differentiation was especially obvious. This may attributed to the difference of these two emulsifiers. As discussed in the previous part, the properties of the two emulsifiers are distinct, which lead to different amount needed in the particle preparation. In the present study, 0.6 g PVA

and 36mg VE-TPGS were used in nanoparticle preparation, respectively. Moreover, the molecular weight of VE-TPGS was much lower than that of PVA. Thus, the remaining VE-TPGS in the particles was much easier to be washed away. It could be concluded that less remaining of the emulsifier lead to less shield of PLGA charge.

Table 5: Zeta-potential of different nanoparticles

Sample	Matrix/Emulsifier/Coating	Zeta-potential
		(mv)
1	PLGA /PVA/--	-13.72
2	PLGA /PVA/Tween 80	-23.13
3	PLGA /PVA/Poloxamer 188	-17.45
4	PLGA /PVA/Poloxamer 407	-21.87
5	PLGA /TPGS/--	-28.5

4.1.3 Drug Loading and Drug Encapsulation Efficiency (EE) of Paclitaxel

The encapsulation efficiency represents the proportion of the initial amount of drug which has been incorporated into the particles. It is an important index for the evaluation of the device, especially for the expensive drugs such as paclitaxel. There are several factors that may affect the encapsulation efficiency of the drug, such as the hydrophobicity of the drug, the size of the particles, and the emulsifier.

High performance liquid chromatography (HPLC) was used to determine the amount of paclitaxel extracted from the nanoparticles. Encapsulation efficiency of the nanoparticles was calculated by equation 1. From the equation it can be seen that to

calculate the original materials used in preparation, only the mass of polymer and drug used in formulation were counted. The mass of the coating materials could not be known clearly because they were absorbed on the particles from the aqueous solution. Thus, only EE of naked particles, sample 1 and sample five were calculated. The results were shown in figure 8 below. Encapsulation efficiency of sample 1, the PVA emulsified nanoparticles, was 46.93%, while that of sample 5, the VE-TPGS, emulsified nanoparticle was 91.14%

$$\text{Encapsulation efficiency (\%)} = \frac{\frac{\text{Mass of drug in nanoparticle}}{\text{Mass of nanoparticle}} \times 100}{\frac{\text{Mass of drug used in formulation}}{\text{Mass of polymer and drug used in formulation}}} \quad (1)$$

In our study, paclitaxel was used as a model drug. It was a highly hydrophobic drug which can be seen from its chemical structure in figure 9. It tends to remain in the oil phase in the process of fabrication. This may explain that the encapsulation efficiency of both samples was relatively high even after repeated washing of the particles in water.

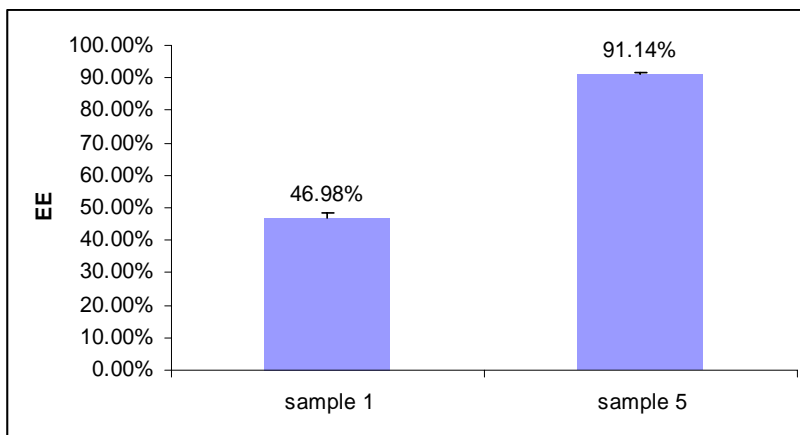


Fig. 8 Encapsulation efficiency of the nanoparticles. Sample 1 is PVA emulsified nanoparticles. Sample 5 is TPGS emulsified nanoparticles.

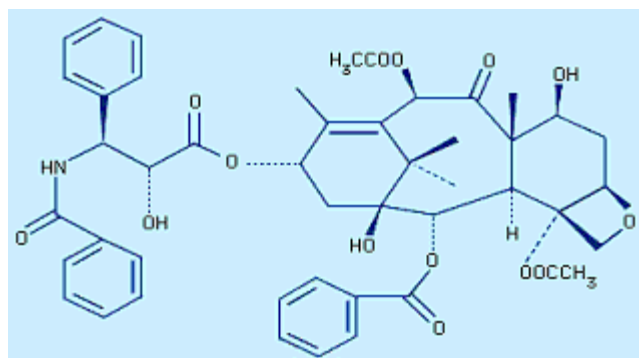


Fig. 9 Chemical structure of paclitaxel

Though the encapsulation efficiency of both sample 1 and sample 5 was relatively high, the values were significantly different. The EE of sample 5 was almost two times of that of sample 1. Considering the size factor, the size of the particles were similar, it could be affect the encapsulation of the paclitaxel significantly. Another factor should be the emulsifier. The advantage of VE-TPGS in increasing the encapsulation efficiency of the particles could be seen. It can also be seen that the EE of the VE-TPGS emulsified nanoparticles was almost two times of that of the PVA emulsified nanoparticles, while the amount of VE-TPGS used was much lower than that of PVA. It has been reported that the EE could even reach 100% when the drug loading ratio was increased to 10% [144]. This achievement significantly improves the solvent evaporation/extraction technique for fabrication of nanoparticles. It is normally difficult to approach such high encapsulation efficiency. The droplet formation, droplet stabilization, nanoparticle hardening is the three essential stages of nanoparticle formation. The formation of solid nanoparticle is brought about by the diffusion of solvent from the emulsion droplet into the continuous phase, followed by the evaporation/extraction of the volatile solvent and the simultaneous inward

diffusion of the non solvent into the droplet. During this course, a partition occurs across the interface from the dispersed phase to the continuous phase. However, the partition is not limited to the organic solvent; both the polymer and the drug molecules may also partition or diffuse across this interface from the organic phase toward the external aqueous phase. The partitioning phenomenon between the dispersed and the dispersing phases contributes to a substantial lowering of microencapsulation yield as well as the encapsulation efficiency. Although the physicochemical characteristic of the drug molecule plays an important role, the surfactant character also has significant effect on the localization of the drug molecule. Modifying the dispersed or dispersing phase of the emulsion by the emulsifier/stabilizer to reduce the leakage of the drug molecule from the oily droplets can thus make improvement of the encapsulation efficiency of the drug in the nanoparticles. In our study, the bulky and large surface area of TPGS resulting from its big lipophilic alkyl tail (polyethylene glycol) and hydrophilic polar head portion (tocopherol succinate) could effectively protect the diffusion or partition of the hydrophobic paclitaxel from polymer to external phase. The encapsulation efficiency of paclitaxel in the polymeric nanoparticle can thus be significantly improved.

As mentioned previously, for those nanoparticles which had been coated by other materials, the EE can not be calculated accurately because the amount of the coating materials in the nanoparticles had not been determined. Thus, drug content was also calculated by equation 2.

$$\text{Drug Content (\% w/w)} = \frac{\text{Mass of drug in nanoparticle} \times 100}{\text{Mass of nanoparticle}} \quad (2)$$

From fig. 10 it can be seen that the drug content ranged from 1.20% to 4.44%. For sample 1 to sample 4, the drug content of particles with coating were lower than that of the particle without coating, this should be resulted from addition of the coating materials on the mass of the particles. Imagine that same amount of naked nanoparticles was prepared, with addition of the coating materials, the mass of the nanoparticle will be increased, and thus the drug content will be decreased. The extent drug content decreased may relatively indicate the amount of coating materials that was adsorbed.

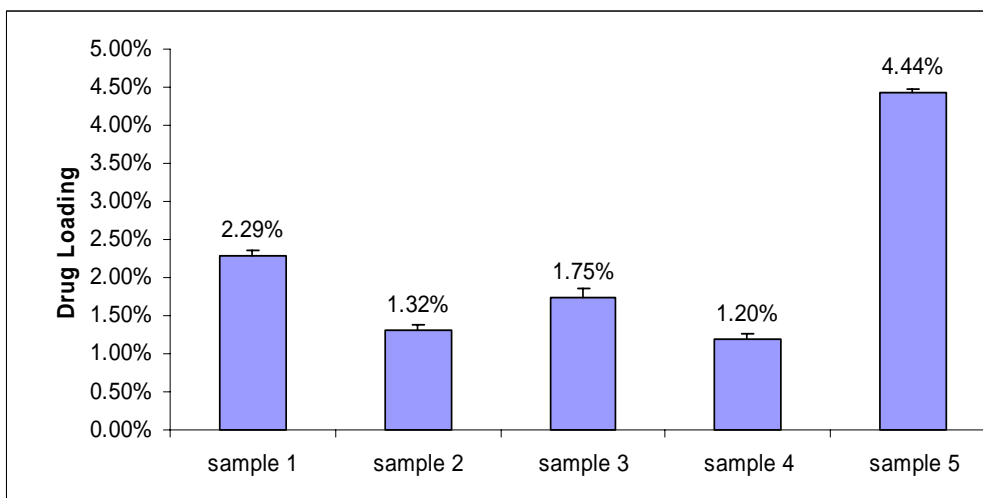
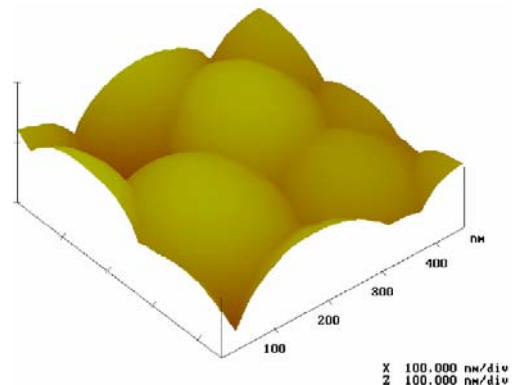
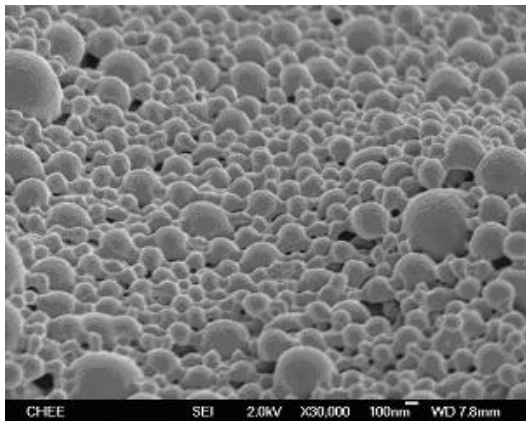


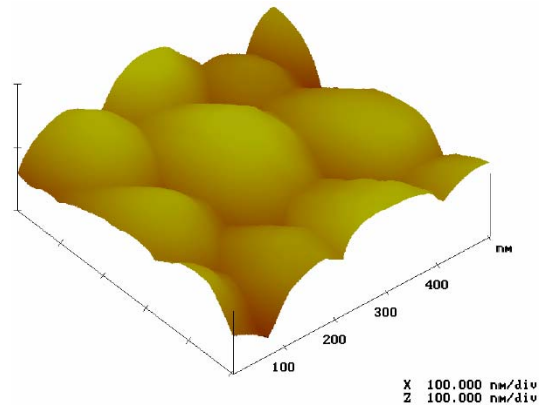
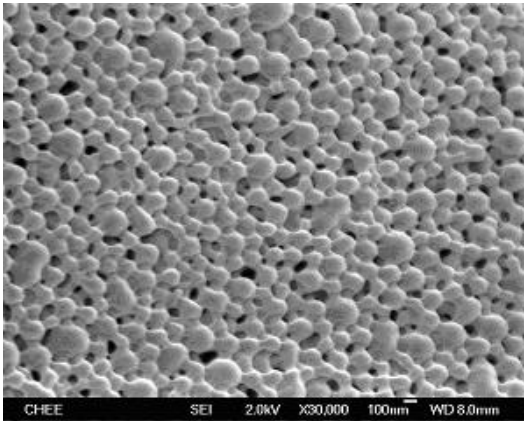
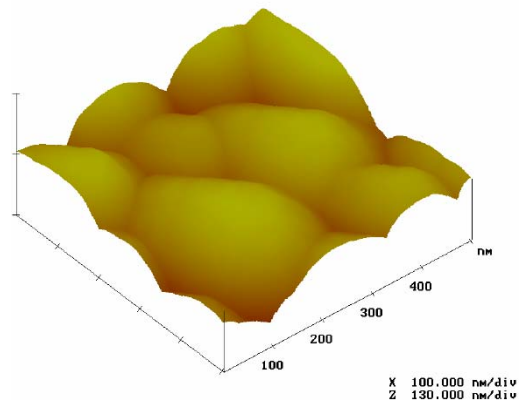
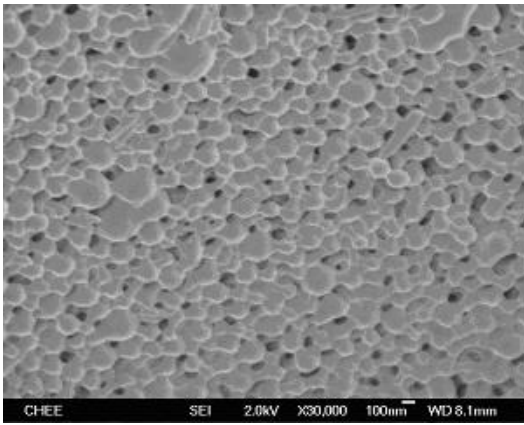
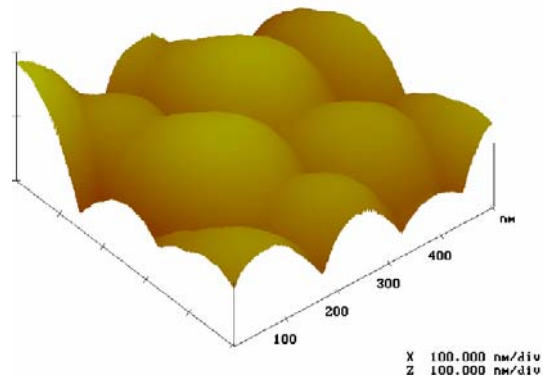
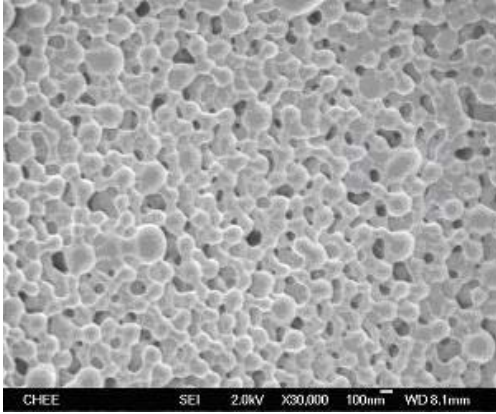
Fig 10 Drug content of the nanoparticles

4.1.4 Morphology

The morphology of the nanoparticles was studied by scanning electrical microscopy (SEM) and atomic force microscopy (AFM). The results were shown in the figures below.

From the SEM picture it can be seen that the nanoparticles had fine spherical shape and smooth surface. The coating seems to have little effect on the morphology of the nanoparticles. There was no aggregation between the particles. AFM technique has been widely applied to provide surface-dependent information in three dimensions on a nanometer scale. It is capable of resolving surface details down to the atomic level and can give morphological images in high resolution. It is not possible to get optimal image for solid nanoparticles in general. The images of the shape and surface characteristic of the nanoparticles were obtained successfully by applying tapping mode AFM. The AFM images reveal the fine structure of the nanoparticles surface. They gave clear 3-D images of spherical nanoparticles and confirmed that there was no aggregation or adhesion among the nanoparticles.





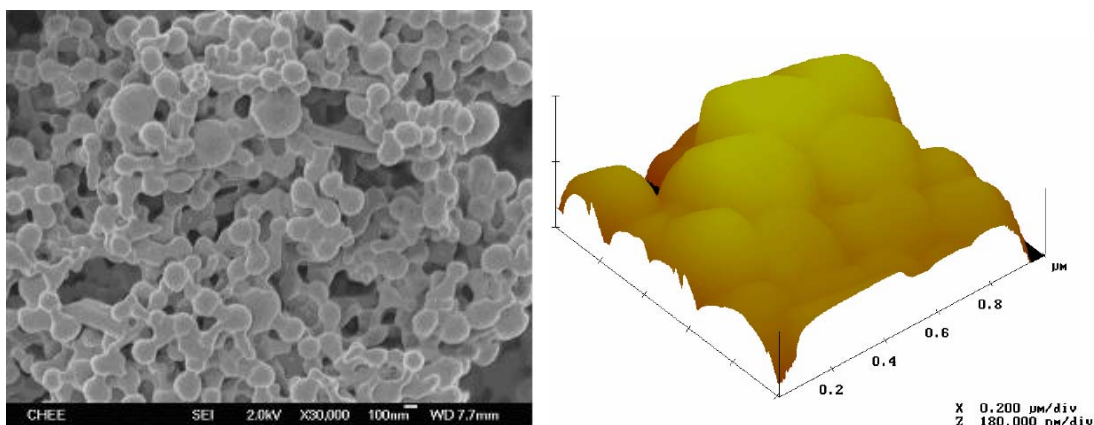


Fig 11 SEM and AFM images of the nanoparticles (from top to bottom: Sample 1, PVA emulsified nanoparticles; sample 2, PVA emulsified Tween 80 coated nanoparticles; sample 3, PVA emulsified poloxamer 188 coated nanoparticles; sample 4, PVA emulsified poloxamer 407 nanoparticles; sample 5, TPGS emulsified nanoparticles).

4.1.5 In Vitro Release of Paclitaxel

In vitro release profile of the drug from the nanoparticles is a very important property of the drug delivery system. One of the main advantages of using nanoparticles to cross the blood brain barrier is that nanoparticles may provide sustained release of drug in the brain to prolong the pharmacological action of drug molecules. The in vitro release experiments may predict behavior of the drug after the nanoparticles is administered to the patients, which included the amount the released drug and time the release may last.

The in vitro release profile of paclitaxel from the nanoparticles was studied by HPLC. The figure below shows the drug release profile in one month when the particles were incubated in PBS at 37°C with shaking. As shown in the figure, sample 1, 2, 3 and 4 are nanoparticles emulsified with PVA. These particles may have similar profile in drug release. They had an initial release burst during the first five days of the release,

which was around 50%. The release gradually decreased and was constant even after one month. At the end of one month, about 60% to 80% drug was released. Their trends were similar. For sample 5, the VE-TPGS emulsified nanoparticle, the rate of drug release was much slower than the PVA emulsified nanoparticles. Also, the initial burst was not as big as that of the PVA emulsified particles.

The diffusion of the drug, the erosion and swelling of polymer matrix and the degradation of polymer are the main mechanisms for the drug release. Since the degradation of PLGA is slow, the release of paclitaxel from the nanoparticles would mainly depend on the drug diffusion and the matrix erosion. In such case, the size, hardness and porosity of the nanoparticles should have significant effects on the release property. The AFM and SEM observation indicated that all the nanoparticles had smooth surface, which supported the slow release of drug by diffusion and matrix erosion mechanism. Moreover, the reason of TPGS emulsified nanoparticles displayed slow release may come from the enhanced interaction or affinity between paclitaxel and polymer matrix. Not only does VE-TPGS possess amphiphilic property, which is necessary for surface-active agents, but it can be dissolved in both the oil and the water phase as well. The TPGS can always be well distributed in water phase or in the oil phase. In addition, the TPGS molecules are bulky and have a large surface area. When forming the emulsion system, TPGS could have the drug and the polymer in a better contact and thus every droplet can be blended thoroughly inside the oil phase. However, PVA does not possess such a property and can thus not be distributed in the oil phase. Nevertheless, further investigations are needed to make a quantitative conclusion.

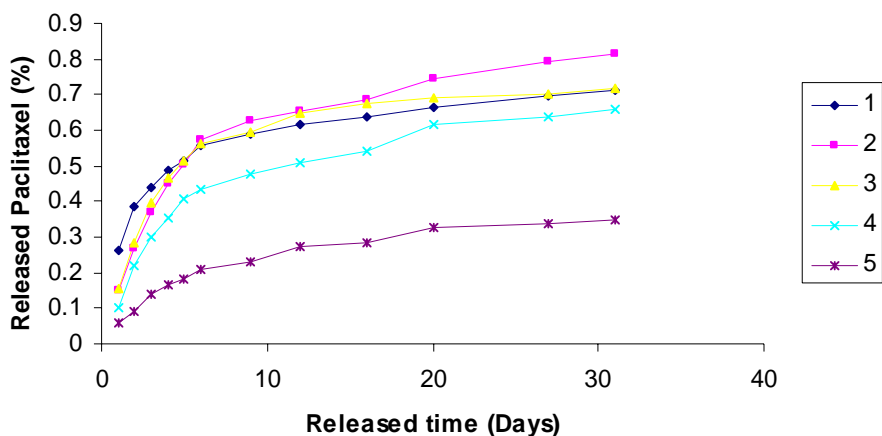


Fig 12 The release profile of paclitaxel from the nanoparticles in PBS

Furthermore, the in vitro release profile demonstrated in PBS buffer could not accurately reveal the real behavior of the drug after the nanoparticles were administered to the patients. In human blood, there are many proteins and molecules which may interact with the nanoparticles and change the profile of drug release. It is necessary to further investigate the release profile of drug from the nanoparticles in serum.

4.1.6 Cell Culture

In vitro evaluation of nanoparticles across the blood brain barrier was carried out using MDCK cells. The blood-brain barrier (BBB) is the tightest barrier known in physiology, for its ability to select and control transported substances. The physical barrier is provided by the endothelial cells, but data has suggested that factors secreted by adjacent cells (astrocytes and pericytes) play a major role in the modulation of cell-cell junctions. MDCK has been used as in vitro models for the BBB as it is endowed with the ability to form polarized monolayers that express tight junctions in the apical side. MDCK cells also produce many of the enzymes found in

the brain endothelial cells. Under appropriate culture condition, monolayers with tightness comparable to that found in the brain endothelial cells, can be obtained within days of culture. MDCK monolayers represent a relatively simple model for the screening of compounds that are transported passively across the blood-brain barrier. Primary brain endothelial cells can also be utilized as a blood-brain barrier screening model for predicting brain permeability. However, the effort required in isolating and characterizing primary brain endothelial cells, along with the batch-to-batch variability of these freshly isolated cells, render this model unattractive for routine use. More consistent results are obtained with cell lines that can be maintained in continuous culture. Since brain endothelial cell lines are not available, alternatives have been developed using other endothelial cells. MDCK cell line is one of them.

Figure 13 shows the morphology of MDCK cells at low (left) and high (high) density. Compared with the bovine brain microvascular endothelial cells (BBMVEC) in figure 14, they had similar morphology.

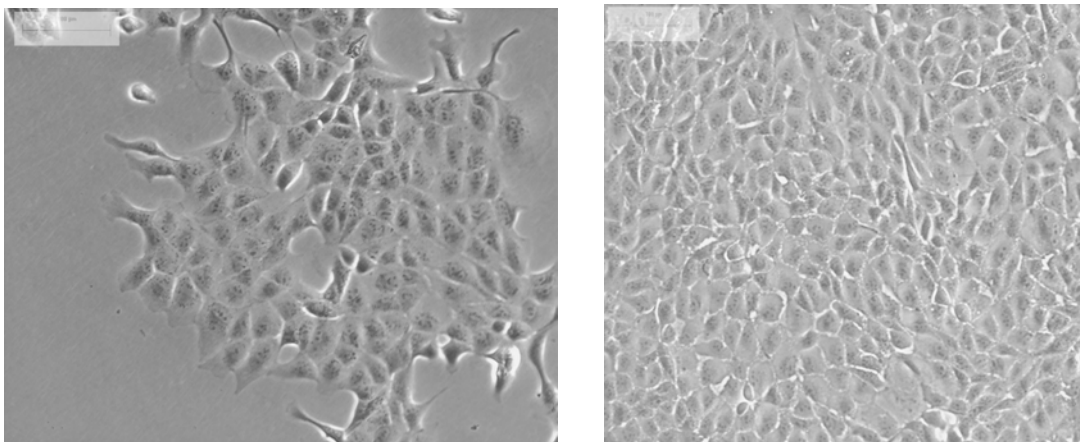


Fig 13 Morphology of MDCK cells at low density (left) and high density (right).

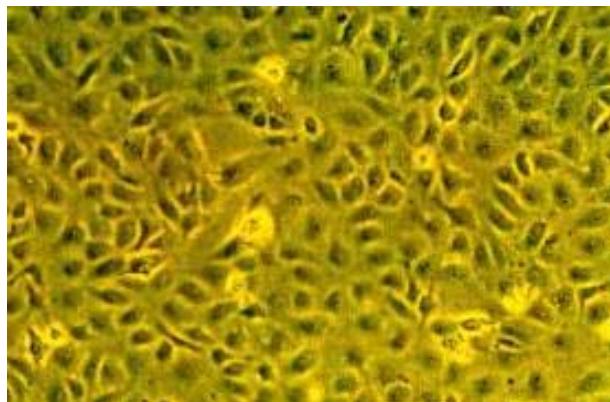


Fig 14 Morphology of bovine brain microvascular endothelial cells (BBMVEC)

4.1.7 Cellular Uptake of Nanoparticles

In order to study cellular uptake of nanoparticles *in vitro* or *in vivo*, the use of fluorescently or radioactively labeled nanoparticles is the most common experimental approach found in the literature. Fluorescent labeling was chosen for the present study to avoid exposure of the samples to the radioactive materials. Fluorescent labeling makes cellular uptake of nanoparticles readily detectable by fluorescence microscopy or CLSM. The extent of particle uptake can then be determined by flow cytometry, fluorometry, or quantitative extraction of the markers from the cells.

As fluorescent markers are sensitive to the environment, their use in nanoparticle visualization can lead to misinterpretation of nanoparticle uptake data due to the leaching or dissociation of fluorescent markers into the released medium and hence subsequently into the cells. Neither could fluorometric analysis differentiate between intracellular and surface located particles, nor determine whether fluorescence detected was due to the cell-associated particles or the fluorescence released from the

particles in the medium which was subsequently taken up by the cells. However, the association of the marker coramarin-6 with the nanoparticles has been demonstrated by in vitro release experiment. It has been shown that only a small part of the markers was released from the particles and the result was believable [145].

In our study, the nanoparticles were washed, freeze-dried and kept in vacuum desiccator after preparation or coating process. The repeated washing process was to ensure that the surface materials adsorbed on nanoparticles were not able to deviate from the particle surface in cell uptake experiments. To carry out cell uptake experiments, the dried fluorescence labeled nanoparticle were dispersed in PBS buffer and incubated with MDCK cells and the particle internalized in the cells were measured by a microplate reader.

As shown in fig. 15 below, 33.5% of sample 1, the PVA emulsified particles, could be internalized in MDCK cells. When coated with Tween 80, poloxamer 188 or poloxamer 407, the uptake could be increased to 53.0%, 51.7 and 61.3%, respectively. For sample 5, the VE-TPGS emulsified nanoparticle, 61.3% particles was internalized, which was almost twice of the naked PVA emulsified particles.

Intracellular uptake of nano- and microparticles has previously been shown to depend on the size and the hydrophobicity of the carrier [132, 146]. In general, the uptake decreases with increasing size and with increasing hydrophilicity. In our study, firstly, it can be seen that PLGA particles below 300 nm was possible to cross the blood brain barrier. This may due to the small size of the particles. Intracellular particulate uptake could either be by phagocytosis or by fluid phase endocytosis [147]. A number

of previous reports have demonstrated phagocytic uptake of nano- and microparticles in macrophages with a lower cut-off size for such a phagocytic uptake being about 0.5um [148]. For nanoparticles of lower size, the main route of intracellular entry is through fluid phase endocytosis. In our study, the size of all the particles was below 300 nm. It may be suggested that the route of uptake may be fluid phase endocytosis. Secondly, it can also be seen that the differences in the surface properties of the formulations have contributed to the difference in uptake. One reason may be the effects of residual PVA on the surface of particles. After coated with other materials, the PVA emulsified nanoparticles increased a lot in intracellular uptake in MDCK cells. This could be attributed shielding of PVA by these materials. It has been reported that relatively high concentration of residual PVA may decrease the intracellular uptake of nanoparticles [149]. Another reason may be the surface hydrophobicities. For the five samples, the surfaces were coated with PVA, Tween 80, poloxamer 188, poloxamer 407, and VE-TPGS. All these molecules were amphiphilic polymers.

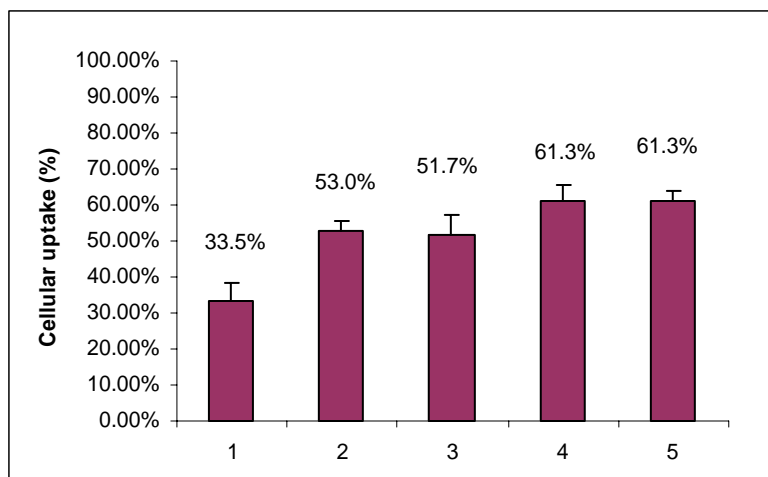
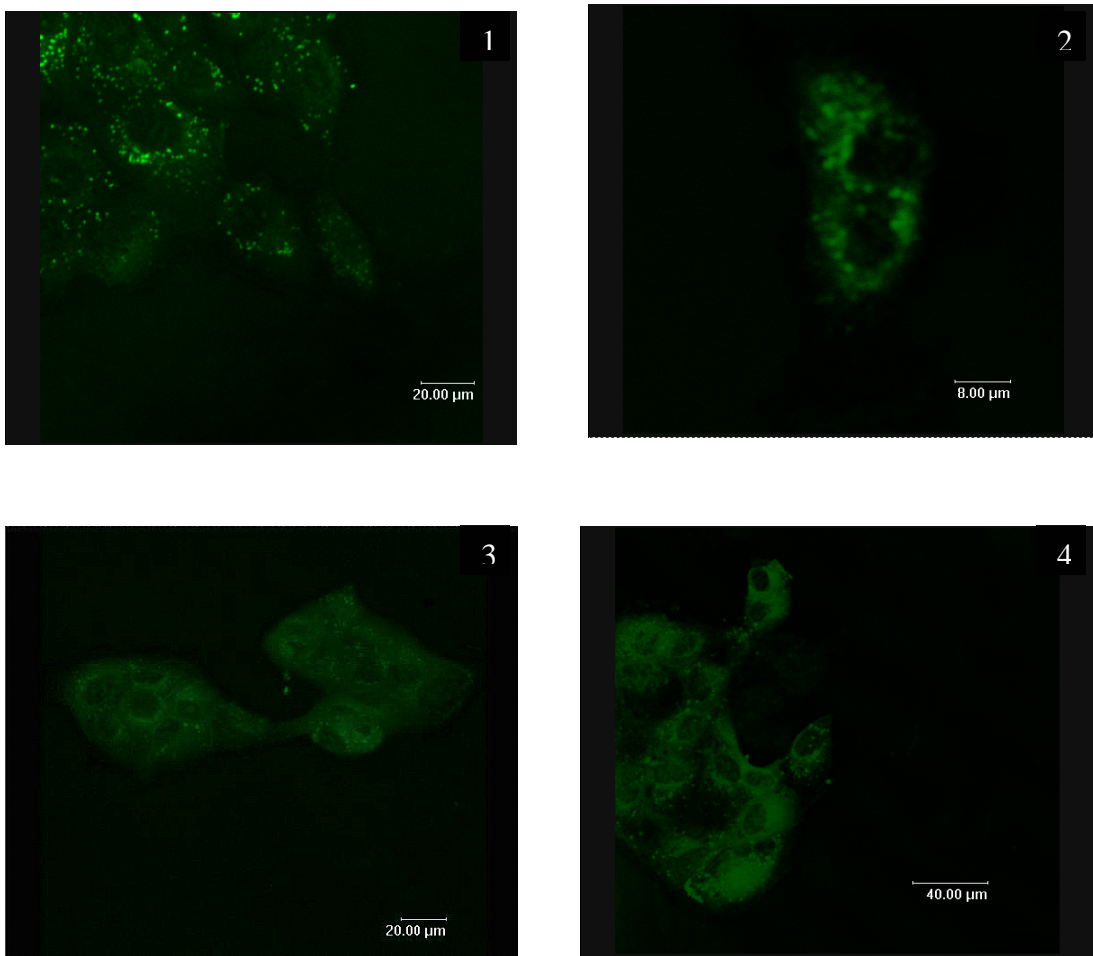


Fig. 15 Cellular uptake of nanoparticles in MDCK cells

To visualize the nanoparticles in the MDCK cells, confocal laser scanning microscopy was employed to take the images of fluorescence labeled nanoparticles incubated with MDCK cells. Figure 16 shows the images of particles internalized in MDCK cells. It can be seen that the particles (in green) were internalized the cytoplasm of the cells.



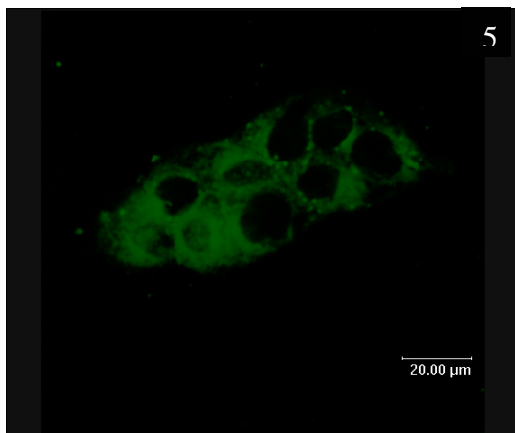


Fig. 16 Confocal laser scanning microscope images of PLGA nanoparticles internalized in MDCK cells (Sample 1, PVA emulsified nanoparticles; sample 2, PVA emulsified Tween 80 coated nanoparticles; sample 3, PVA emulsified poloxamer 188 coated nanoparticles; sample 4, PVA emulsified poloxamer 407 nanoparticles; sample 5, TPGS emulsified nanoparticles)

4.2 GD-DTPA LOADED NANOPARTICLES OF BIODEGRADABLE POLYMERS FOR MRI OF THE BRAIN

4.2.1 Particle Size

PLGA and PLA-PEG were used to prepare nanoparticles by nanoprecipitation method. Totally four batches of samples were prepared. Sample 1 was prepared using PLGA. Sample 2 and 3 was prepared using PLA-PEG (90:10) with different concentration of the polymer. Sample 4 was prepared using PLA-PEG (70:30). Particle size was determined by laser light scattering. The results are mean value of 6 measures.

Size and size distribution play important roles determining the fate of the nanoparticles after administration. Especially for crossing the blood brain barrier, smaller size is preferred. As discussed previously, particles smaller than 100 nm are ideal for crossing the blood brain barrier. However, particle size also affects the encapsulation efficiency of the drug. Usually, the size is smaller, the EE is lower. This is because that the small particles have a high surface area compared to their volume and a high proportion of the drug which is incorporated will be at or near the surface of the nanoparticles and can be readily released during nanoparticle production or during the removal of unincorporated drug.

Table 6 shows the results of size and size distribution of the particles. From the results of particle size it can be found the size of these particles were very small. Except sample 1, the PLGA nanoparticles, all the other samples were less than 100 nm, which were very suitable for crossing the blood brain barrier. This could be attributed to the structure of the polymer. It can be seen that the proportion of PEG in the polymer played an important role in determining the size of the particle. The larger the PEG proportion, the smaller the size was. This may due to the hydrophobicity of the polymer. In the process of particle fabrication by nanoprecipitation, the nanoparticles were formed by the interfacial turbulence resulted from the rapid diffusion of water miscible solvent to the water. The energy released in this diffusion process provides the formation of the particles [150-152]. The faster the diffusion is, the smaller the particle size would be. For this kind of polymer, the part of PLA is hydrophobic and the part of PEG is hydrophilic. With more PEG part, the diffusion rate of the polymer solution into the water should be

faster. This may explain why the particle size of sample 4, PLA-PEG (70:30) particle, was much smaller than that of sample 3 PLA-PEG (90:10) particle while other conditions were similar.

Furthermore, the concentration of the polymer solution also affected the size of the particles. The size of sample 2, with the polymer concentration of 0.94% (w/v), was 16.1 nm smaller than that of sample 3, with the polymer concentration of 1.5%. This was due to the same reason, the diffusion rate of the polymer solution in the water phase. When the concentration of the solution was increased, the viscosity of the solution was also increased, which made the diffusion rate of the polymer into the water slower.

Table 6: *The size and polydispersity of the Gd-DTPA loaded particles*

Sample	Polymer : Solvent	Size	Polydispersity
1	PLGA (75mg) : Acetone (8ml)	284.8±5.9	0.136±0.034
2	PLA-PEG (90:10) (75mg) : Acetone (8ml)	83.2±0.7	0.169±0.025
3	PLA-PEG (90:10) (75mg) : Acetone (5ml)	99.3±1.1	0.215±0.011
4	PLA-PEG (70:30) (75mg) : Acetone (5ml)	81.0±5.5	0.236±0.028

4.2.2 Morphology

The morphology of the Gd-loaded particles was investigated by SEM. The image of PLGA nanoparticles was shown in fig 17; the image of PLA-PEG nanoparticles was shown in fig. 18.

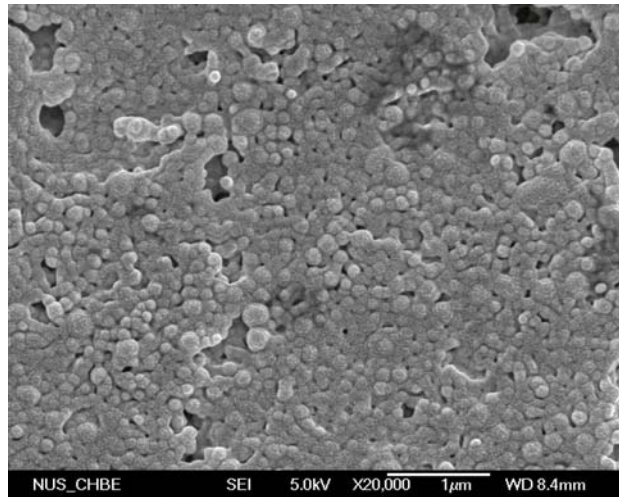


Fig 17 SEM image of PLGA nanoparticle

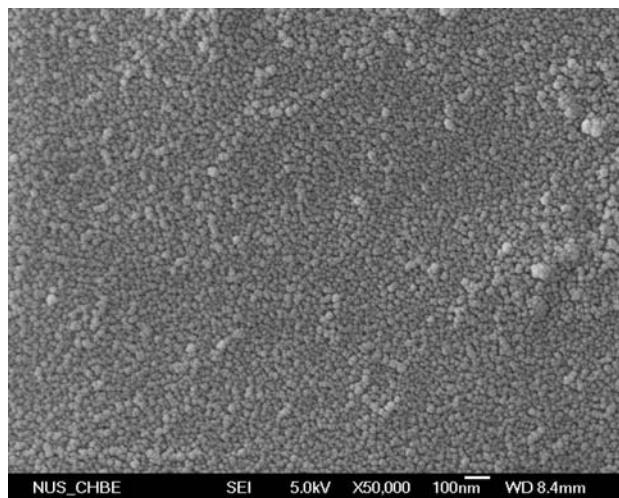


Fig 18 SEM image of PLA-PEG nanoparticles

From the picture it can be found that the morphology of PLGA nanoparticles was different from that of the particles made by single emulsion solvent evaporation methods although their size was similar. It can be seen that there were aggregations among the particles. This may be due to the difference of the manufacturing process. In the nanoprecipitation method, only 100 mg F-68 was used dissolved in the water

phase and it could be more easily washed away than PVA or VE-TPGS in the centrifugation step. Thus, after freeze dry, the particles may be aggregated because there was less remaining surfactant or coated materials on the particle surface.

Compared the PLGA and PLA-PEG nanoparticles, there were differences between the two samples. Firstly, as reflected in the result of the laser light scattering study, their size was different. The PLGA particles were much larger than the PLA-PEG particles. Secondly, there was no significant aggregation in PLA-PEG particles compared with the PLGA nanoparticles.

It can also be seen from the picture that the size of PLA-PEG nanoparticles was less than 50 nm. This may attribute to the process of freeze drying. The lose of water from the particles made them smaller than measured in suspension by laser light scattering.

4.2.3 Loading and Encapsulation Efficiency of Gadolinium

The amount of Gd-DTPA extracted from the nanoparticles was determined by ICP-AES. The results are shown in the table below. The results are mean value of three measures.

Encapsulation efficiency and drug content are important factors to be considered. A nanoparticle system with high encapsulation efficiency and drug content will reduce the quantity of carrier required for the administration of sufficient amount of active compound to the target site as well as drug wastage during manufacturing. However, for all the water soluble drugs, a big problem is the poor encapsulation efficiency and

drug content. The low encapsulation efficiency and drug content are mainly due to rapid migration of the drugs from the particles to the external aqueous phase.

In our study, Gd-DTPA was used to label the nanoparticles and facilitate the visualization of particles by the MRI. In the MRI imaging experiment, the amount of gadolinium needed in one experiment is fixed. Therefore, high encapsulation efficiency and drug content were very important because they would lead to less usage of nanoparticles in one injection. This will also make the injection quicker and easier.

As the results shown in table 7, the encapsulation efficiency of gadolinium was very low. Sample 2 and 3 had EE of 1.79% and 3.63%. This means that almost all of the Gadolinium leaked from the particles into the water. EE of sample 4 was 12%. Even for this sample, most of the Gadolinium migrated from the particles into the water phase. From the results it can be seen that the hydrophilic nature of Gd-DTPA resulted in a significant loss of the drug to the external aqueous phase during the production process. Compared sample 3 and 4, it can be seen that the structure of the polymer also affected the EE of the nanoparticles. The EE of sample 4 was about 3.3 times of that of sample 3. This may be due to the hydrophilicity of polymer. Sample 4 was made up of PLA-PEG (70:30) while sample 3 is made up of PLA-PEG (90:10). The PEG part in the polymer was hydrophilic. The drug was also hydrophilic. There may be more interactions between the polymer and the drug, which led to a higher encapsulation efficiency. Furthermore, the effects of particle size on the encapsulation efficiency could also be seen from the results. From the results of size, the sequence

of size from large to small was sample 3, sample 2, and sample 4. In the results of encapsulation efficiency, the sequence was reversed. This was because that the small particles have a high surface area compared to their volume so that a high proportion of the drug which is incorporated will be at or near the surface of the nanoparticles and this part of the drug can be readily released during nanoparticle production.

For sample 1, the PLGA nanoparticle, the content of drug in the particle was not uniform among the triplicate samples and can not be determined accurately.

Table 7: *Encapsulation efficiency and drug content of the Gd-DTPA loaded nanoparticles*

Sample	Polymer : Solvent	Encapsulation Efficiency (%)		Drug loading (%)	
		Gd	Gd-DTPA	Gd	Gd-DTPA
2	PLA-PEG (90:10): Acetone (8ml)	1.79	2.45	0.26	0.92
3	PLA-PEG (90:10): Acetone (5ml)	3.63	4.96	0.53	1.86
4	PLA-PEG (70: 30) : Acetone (5ml)	12.00	16.37	1.76	6.14

4.2.4 In Vitro Release of Gadolinium

In vitro release of Gd-DTPA is an important profile that must be demonstrated before the animal study. It can give out a rough prediction on the fate of gadolinium after the nanoparticles were injected in the animals. Gd-DTPA will be imaged by the MRI whether it is incorporated in the nanoparticle or released from the particles. Thus, it is

necessary to get the prediction of the release profile from the particles so that the image can be analyzed objectively.

Figure 19 shows the release profile of gadolinium from the particles. Sample 3 and sample 4 were chosen for this characterization because they had relatively high encapsulation efficiency and may be used for further experiments. From the results it can be seen that for both samples small part of the drug was released in 24 hours. The rate of release was slow. For sample 3, about 15% of the gadolinium was released in 3 hours and after that about 20% of the gadolinium was released in 21 hours. For sample 4, about 5% of the gadolinium was released in 3 hours and less than 10% of the gadolinium was released in 21 hours. For both samples, there was a small initial burst in the first 3 hours and after that, the release rate was quite slow. This release profile may be favorable in MR imaging.

However, the in vitro release profile demonstrated in PBS buffer could not accurately reveal the real behavior of gadolinium after the nanoparticles were administered to the animals. There are many proteins and molecules in the blood which may interact with the nanoparticles and change the profile of gadolinium release. It is necessary to

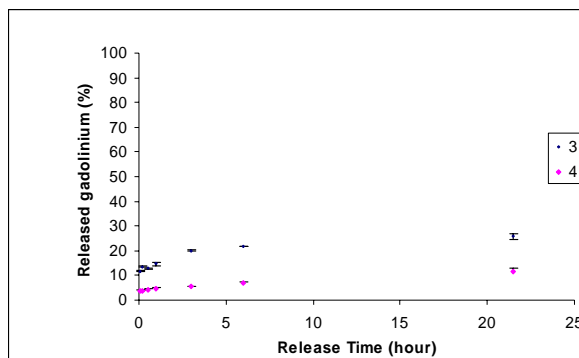


Fig 19 Release of gadolinium from the nanoparticle further investigate the release profile of drug from the nanoparticles in serum.

CHAPTER FIVE

CONCLUSIONS AND FUTURE WORK

5.1 CONCLUSION

In this study, nanoparticles of biodegradable polymer were prepared as a drug delivery device to cross the blood brain barrier. PLGA particles below 300 nm were made by single emulsion solvent evaporation method. Paclitaxel, a model drug, had relatively high encapsulation efficiency in the particles. The surface properties of the particles were modified by coating the surface with tween 80, poloxamer 188 and poloxamer 407 or by changing the usually used emulsifier PVA to a natural biomolecule, VE-TPGS. After modification, the surface charge of the particles was changed. More importantly, the cellular uptake of the particles in monolayer of MDCK cells was increased from 30% to about 50% or 60%. The internalization of the nanoparticles in MDCK cells were proved by confocal laser scanning microscopy. From the in vitro cell work it may be concluded that using nanoparticles of biodegradable polymers to penetrate the blood brain barrier is feasible. And the size and surface properties of the nanoparticles play key roles. To carry out animal studies, Gd-DTPA PLA-PEG nanoparticles were prepared by nanoprecipitation method. Nanoparticles around 100 nm were obtained. ICP-AES were employed to measure the amount of gadolinium in the particles. It was found the polymer played important roles in determining the content of gadolinium in the particles. In vivo experiment on rat has been designed and will be carried out.

5.2 FUTURE WORK

In this work, we have demonstrated on cell level that it is feasible to use nanoparticles of biodegradable polymers to cross the blood brain barrier. And the particles for animal study were almost ready to be used. To further investigate the feasibility of nanoparticles to cross the blood brain barrier and their distribution in the brain of the animals, animal study should be carried out by MRI. Due to the time limitation, the work will be continued to the fellow students.

REFERENCE

1. Enrich, P. Das Sauerstoff-Bedurfnis des Organismus. Eine Farbenanalytische Studies. Berlin: hirschwald, 1885
2. Goldmann, E. Beitr Klin Chirurg 64: 192-265, 1909
3. Aschner, Kerper, Mol. Biol. and Tox. of Metals, 2000
4. Reese, T.S., Karnovsky, M., J. cell boil., 40: 648-77, 1969
5. Brightman, M. W., Reese, T.S., J Cell Biol 40: 648-677, 1969
6. Brightman, M. W., Exp. Eye Res., 25 (suppl.): 1-25. 1977
7. Brightman M., Handbook of experimental pharmacology 103, Springer-Verlag, Berlin, 1-22, 1992.
8. Lo, E.H., Singhal, A.B., Torchilin, V.P., and Abbott N.J., Brain Res Rev, 38:140-148, 2001.
9. Kroll RA, Neuwelt EA, Neurosurgery 42: 1083-1100, 1998
10. Neuwelt EA , New York: plenum press, Vols 1 and 2, 1989
11. Brightman MV, Hori M, Rapoport SI, J comp Neurol 152: 317-325, 1973
12. Rapoport SI, Robinson PJ, Ann NY Acad Sci 481: 250-267, 1986
13. Lee, G.; Dallas, S.; Hong, M.; Bendayan. R. Pharmacol. Rev., 53: 569-96, 2001
14. Fromm, M. F. Int. J. Clin. Pharmacol. Ther. 38: 69-74, 2000
15. Lorris Betz, An overview of the multiple functions of the blood-brain barrier, in Bioavailability of Drugs to the Brain and the Blood-Brain Barrier, National Institute on Drug Abuse, Research Monograph Se
16. Ohnishi T, Tamai I, Sakanaka K, Sakata A, Yamashima T, Yamashita J and Tsuji A Biochem Pharmacol 49: 1541-1544, 1995
17. Mankhetkorn S, Dubru F, Hesschenbrouck J, Fiallo M, Garnier-Suillerot A Mol Pharmacol 49: 532-539, 1996
18. Loo T.W., and Clarke, D.M. Biochem. Cell Biol. 77: 11-23, 1999
19. Ambikanandan Misra, Ganesh s., Aliasgar Shahiwala, Shrenik P. Shah, J pharm Pharmaceut Sci 6 (2): 252-273, 2003
20. P.R. lockman, R.J. Mumper, M. A. Khan, and D.D. Allen, Drug development and industrial Pharmacy, 28 (1): 1-12, 2002.
21. S.V. Vinogradov, T.K. Bronich, A.V. Kabanov, Adv. Drug Del. Rev. 54: 223-233, 2002
22. <http://www.abc.net.au/science/k2/moments/s981339.htm>
23. Witt KA, Gillespie TJ, Huber JD, Egleton, R.D., and Davis, T.P., Peptides, 22: 2329-2343, 2001
24. Siegal, T. and zylber-Katz, E., Clin Pharmacokinet, 41:171-186, 2002.

25. Habgood, M.D., Begley, D.J. and Abbott, N.J., *Cell Mol Neurobiol*, 20:231-253, 2000.
26. Thorne, R.G. and Frey II, W.H., *Clin Pharmacokinet*, 40:907-946, 2001.
27. Filmore, D., *Modern Drug Discov*, 5:22-27, 2002.
28. Madrid, Y., Langer, L.F., Brem, H. and Langer, R., *Adv Pharmacol*, 22:299-324, 1991
29. Bodor, N. and Kaminski, J.J., *Annu Rep Med Chem*, 22:303–313, 1987.
30. Lambert, D.M., *EurJ Pharm Sci*, 11:S15-27, 2000.
31. Han, H.k and Amidon, G.L., *AAPS PharmSci*, 2:E6, 2000.
32. Bodor, N. and Buchwald, P., *Pharmacol Ther* 76:1–27, 1997
33. Palomino, E., Kessel, D. and Horwitz, J.P., *J Med Chem*, 32:622–625, 1989.
34. Takada, Y., Vistica, D.T., Greig, N.H., Purdon, D., Rapoport, S.I. and Smith, Q.R., *Cancer Res*, 52:2191–2196, 1992.
35. Pardridge, W.M., *Nat Rev Drug Discov*, 1:131-139, 2002.
36. Pardridge, Raven Press, NY, 1–357, 1991.
37. Bickel, U., Yoshikawa, T., Landaw, E.M., Faull, K.F. and Pardridge, W.M., *Proc Natl Acad Sci*, 90:2618–2622, 1993.
38. Lodish, H.F. and Kong, N., *J Biol Chem*, 268:20598–20605, 1993.
39. Yoshikawa, T. and Pardridge, W.M., *J Pharmacol Exp Ther*, 263:897–903, 1992.
40. Neuwelt, E.A. and Dahlborg, S.A., Vol. 2, Plenum Press, New York, 195–262, 1989.
41. Neuwelt, E.A., Williams, P.C., Mickey, B.E., Frenkel, E.P. and Henner, W.D., *Pediatr Neurosurg* 21:16–22, 1994.
42. Doran, S.E., Ren, X.D., Betz, A.L., Pagel, M.A., Neuwelt, E.A., Roessler, B.J. and Davidson, B.L., *Neurosurgery*, 36:965–970, 1995.
43. Neuwelt, E.A., Weissleder, R., Nilaver, G., Kroll, R.A., Roman-Goldstein, S., Szumowski, J., Pagel, M.A., Jones, R.S., Remsen, L.G. and McCormick, C.I., *Neurosurgery*, 34:777–784, 1994.
44. Hiesiger, E.M., Voorhies, R.M., Basler, G.A., Lipschutz, L.E., Posner, and Shapiro, W.R., *Ann Neurol*, 19:50–59, 1986.
45. Chio, C.C., Baba, T. and Black, K.L., *J Neurosurg*, 77:407–410, 1992.
46. Black, K.L., Baba, T. and Pardridge, W.M., *J Neurosurg*, 81(5):745–751, 1994.
47. Matsukado, K., Inamura, T., Nakano, S., Fukui, M., Bartus, R.T. and Black, K.L., *Neurosurgery*, 39:125–133, 1996.
48. Harbaugh, R.E., Saunders, R. L. and Reeder, R.F., *Neurosurgery*, 23(6):693-698, 1988

49. Thorne, R.G., Emory, C.R., Ala, T.A. and Fery, W.H., *Brain Res*, 692(1-2):278-282, 1995
50. Born, j., Lange, T. and Kern, W., *Sniffing*, *Nat Neurosci*, 5:514-516, 2002
51. Illum, L., *Drug Discov Today*, 7:1184-1189, 2002
52. Bobo, R.H., Laske, D.W., Akbasak, A., Morrison, P.F., Dedrick, R.L. and Oldfield, E.H., *Proc Natl Acad Sci U.S.A.*, 91:2076-2082, 1994.
53. Neuwelt, E.A., Kroll, R.A., Pagel, M.A., Muldoon, L.L and Roman Goldstein, S., *Neurosurgery*, 38(4):1129-1145, 1996.
54. Brem, H. and Langer, R., *Sci Med*, 3(4):1-11, 1996
55. Brem, H. and Gabikian, P., *J Control Release*, 74:63-67, 2001
56. Yurek, D.M. and Sladek, J.R., *Annu Rev Neurosci*, 13:415-440, 1990
57. P.R. lockman, R.J. Mumper, M. A. Khan, and D.D. Allen, *Drug development and industrial Pharmacy*, 28 (1), 1-12, 2002
58. Y. Chen, G. Dalwadi and H.A.E. Benson, *Current drug delivery*, 1,000-000.,2004
59. Olivier, J. C., Fenart, L., Chauvet, R., Pariat, C., Cecchelli, R. , Couet, W. *Pharm. Res.*, 16, 1836-42, 1999
60. K. Park, *Controlled Drug Delivery: Challenges and Strategies*, American Chemical Society, Washington, DC, 1997
61. A. Carrio, G. Schwach, J. Coudane, M. Vert, *J. Controlled Res* 37 113-121, 1991
62. J. kreuter, Renad N. Alyautdin, Dimitri A. Kharkevich, Alexei A. Ivanov, *Brain research* 674, 171-174, 1995
63. J. Kreuter, V.E. Petrov, d.A. Kharkevich, R.N. Alyautdin, *Journal of Controlled Release* 49, 81-87, 1997
64. Jorg Kreuter, Peter Ränge, Valery Petrov, Stefan Hamm, Svetlana E. Gelperina, Britta Engelhardt, Renad Alyautdin, Hagen Von Briesen, and Vadid J. Begley, *Pharmaceutical Research*, Vol. 20, No. 3, 2003
65. Schröder, U., Schröder, H. & Sabel B. A. *Life Science* 66, 6: 495-502
66. L. Illum, L.O. Jacobsen, R.H. Muller, E. Mak and S.S. Davis, *Biomaterials* 8 113-117, 1987
67. L. Illum, S.S. Davis, R.H. Muller, E. Mak and P. West, *Life Sci.* 40 367-374, 1987
68. Mu, L., Feng, S.S., *J Control Release.* 71, 53-69, 2001
69. Mu, L., Feng, S.S. *J Control Release.* 80(1-3), 129-144, 2002
70. Mu, L., Feng, S.S. *J Control Release.* 86(1):33-48, 2003
71. Feng, S.S, Mu, L., Khin YW, Huang GF, *Current medicinal chemistry*, 11, 413-424, 2004

72. Kroger, N., Achterrath, W. Hegewisch-Becker, S., Mross, K., and Zander, A. R. *Cancer Treat. Rev.* 25: 279-291, 1999
73. Nathan, F. E., Berd, D., Sato, T., and Masrangelo, M. J. *Cancer.* 88: 79-87. 2000.
74. Muggia, F. M, *J. Clin. Oncol.* 18: 106-115, 2000
75. Papadimitriou, C. A. *Cancer.* 89: 1547-1554, 2000
76. Belani, C. P. *Chest.* 117 (Suppl 1): 144S-151S, 2000
77. Lee, J. S., *Sem. Oncol.* 24 (4 Suppl. 12): S12/52-S12/55, 1997
78. Glantz, M. J., Chamberlain, M. C., Chang, S. M., Prados, M. D., and Cole, B. F. *Sem. Rad. Oncol.* 9: 27-33, 1999
79. Brandes, A.A., Pasetto, L.M., and Monfardini, S. *Anticancer Res.* 20: 1913-1920, 2000
80. Eiseman, J. L., *Cancer Chemother. Pharmacol.* 34: 465-471, 1994
81. Heimans, J. J., *Ann. Oncol.* 5: 951-953, 1994
82. Stephan Fellner, *J. Clin. Invest.* 110: 1309-1318, 2002
83. Webster's revised unabridged dictionary (1913)
84. WHO website, <http://www.who.int/cancer/en/>
85. Estimated new cancer cases and deaths for 2003, SEER Cancer Statistics Review 1975-2000, National Cancer Institute
86. WHO website, Country situation and trends, geography, demographic statistics, China, People's Republic of.
87. WHO website, country situation and trends, geography, demographic statistics, Singapore
88. Oncology: treatment and management. Part 2, Cancer treatment. Pharmaceutical representative, November 2002
89. Feng S.S., Chien S., *Chemical Engineering Science* 58, 4087-4114, 2003
90. Paul Ehrlich, *Lancet, London,* 2: 445-451, 1913
91. Cancer FAQs about chemotherapy, frequently asked questions about common cancers, National Foundation for Cancer Research
92. Lisa Brannon-Peppas, *Polymers in controlled drug delivery.*
93. L. Mu, S.S. Feng, *Journal of controlled release* 86, 33-48, 2003
94. A primer of brain tumors, brain tumor basics (chapter 2), American Brain Tumor Association.
95. <http://www.neurologychannel.com/nstumors/types.shtml>, neurology channel, nervous system tumors.
96. A primer of brain tumors, Facts and statistics (chapter 3), American Brain Tumor Association.

97. Treatment, National Brain Tumor foundation
98. S.V. Vinogradov, T.K. Bronich, A.V. Kabanov, *Adv. Drug Del. Rev.* 54 223-233, 2002
99. W. Zauner, N.A. Farrow, A.M. Haine, *J. Control. Release* 71, 39-51, 2001
100. Uday B. Kompella, Nagesh bandi, Surya P. Ayalasomayahula, *Drug delivery technology* , volume 1, no. 1, 2001
101. Hideki Murakami, a, Masao Kobayashia, Hirofumi Takeuchib and Yoshiaki Kawashimab, *International journal of pharmaceutics*, 187, 2, 143-152 , 1999
102. Prokop A, Holland CA, Kozlov E, Moore B, Tanner RD *Biotechnol Bioeng* 75:228-232, 2001
103. Quintanar-Guerrero D., Allémann E, Doelker E., Fessi H., *Polymer and Colloid Science*, (275) 640-647,1997
104. Gangadhar Sunkara, M Pharm, and Uday B. Kompella, *Drug delivery technology*, Vol. 2 No.1, 2002
105. Lakkireddy, H.; Rayasa. R., *Acta Pharm.* 54 103-118, 2004
106. D. Graiver and A.W. Lomas, US Patent 5,629,401, May 13, 1997
107. Ulbrich, K.; Strohmalm, J. ; Subr. V.; Plocova, D.; Duncan. R.; Rihova. B. *Macromol. Symp.* 103, 177, 1996
108. Putnam., D. A.; Shiah, J. G. ; Kopecek, J. *Biochem. Pharmacol.* 52. 957, 1996
109. Ulbrich, K.; Subr, V.; Podperova, P.; Buresova, M. J. *Controlled Release* 34, 155, 1995
110. Krinick, N.L.; Sun, Y.; Joyner, D.; Spikes, J.D.; Straight, R.C.; Kopecek, J. J. *Biomater. Sci., Polyma. Ed.* 1994
111. Heller, J.; Sparer, R.V.; Zentner, G.M. In *Biodegradable Polymers as Drug Delivery System*; Chasin, M.; Langer, R. Eds.; Marcel Dekker; New York, 1990
112. Lan, P.N.; Corneillie, S.; Schacht, E.; Davies, M.; Shard, A. *Biomaterials* 17, 2273, 1996
113. Kimura, Y.; Makita, Y.; Kumagai, T.; Yamane, H.; Kitao, T.; Sasatani, H.; Kim, S.I. *Polymer* 33, 5294, 1992
114. Yeh, P.; Kopeckova, P.; Kopecek, J. *Macromol. Chem. Phys.* 196, 2183, 1995
115. Schierholz, J.M.; Rump, A.; Pulverer, G. *Drug Res.* 1997, 47
116. *Journal of biomedical materials research*, volume 50, issue 3, 388-396
117. Kricheldorf, H. R.; Meierhaack, J. *Makromol. Chem.sMacromol. Chem. Phys.* 194, 715-725, 1993
118. Chen, X.; McCarthy, S. P.; Gross, R. A. *Macromolecules* 30, 4295-4301, 1997
119. Deng, X. M.; Xiong, C. D.; Cheng, L. M.; Xu, R. P. J. *Polym. Sci., Part C: Polym. Lett.* 1990, 28, 411-416

120. Rashkov, I.; Manolova, N.; Li, S. M.; Espartero, J. L.; Vert, M. *Macromolecules* 29, 50-56, 1996
121. Li, S. M.; Rashkov, I.; Espartero, J. L.; Manolova, N.; Vert, M. *Macromolecules* 29, 57-62, 1996
122. Li, Y. X.; Kissel, T. J. *Controlled Release* 27, 247-257, 1993
123. Agrawal, C. M.; Athanasiou, K. A.; Heckman, J. D. *Mater. Sci. Forum* 1997, 250, 115-128.
124. Gref R, Domb A, Quellec P, Blunk T, M. Uller RH, Verbavatz JM, Langer R. *Adv Drug Deliv Rev.* 16: 215-33, 1995
125. Kwon GS, Kataoka K. *Adv Drug Deliv Rev* 16:295–309, 1995
126. Torchilin VP, Papisov MI J, *Liposomes Res* 4:725–39, 1994
127. Blume G, Cevc G. *Biochim Biophys Acta* 1146:157–68, 1993
128. Fenart, L.; Casanova, A.; Dehouck, B.; Duhem, C.; Slupek, S.; Cecchelli, R.; Betbeder, D. *J. Pharmacol. Exp. Ther.*, 291, 1017-22, 1999
129. Fundaro, A.; Cavalli, R.; Bargoni, A.; Vighetto, D.; Zara, G. P.; Gasco, M. R. *Pharmacol. Res.*, 42, 337-43, 2000
130. Lockman, P. R.; Oyewumi, M. O.; Koziara, J. M.; Roder, K. E.; Mumper, R. J.; Allen, D. D. *J. Control Release*, 93, 271-282, 2003
131. Yuan F, Leuning M, Huang SK, Berk DA, Papahadjopoulos D, Jain RK. *Cancer Res* 54: 3352-6, 1994
132. Desai MP, Labhasetwar V, Walter E, Levy RJ, Amidon GL. *Pharm Res* 14: 1568-73, 1997
133. Moghimi SM, Porter CJH, Muir IS, Iillum L, Davis SS. *Biochem Biophys Res Commun* 177: 861-6, 1991
134. Kwon GS, Kataoka K. *Adv Drug Deliv Rev* 16: 295-309, 1995
135. Konan YN, Gurnery R, Allemann E, *Int J Pharm* 233: 239-52, 2002
136. Fundaro, A.; Cavalli, R.; Bargoni, A.; Vighetto, D.; Zara, G. P.; Gasco, M. R. *Pharmacol. Res.*, 2000, 42, 337-43
137. Friese, A.; Seiller, E.; Quack, G.; Lorenz, B.; Kreuter, J. *Eur. J. Pharm. Biopharm.*, 2000, 49, 103-9
138. Alyaudtin, R. N.; Reichel, A.; Lobenberg, R.; Ramge, P.; Kreuter J.; Begley, D. *J. J. Drug Target*, 2001, 9, 209-21
139. Calvo, P.; Gouritin, B.; Brigger, I.; Lasmezas, C.; Deslys, J. Williams, A.; Andreux, J. P.; Dormont, D.; Couvreur, P. *Neurosci. Methods*, 2001, 111, 151-5
140. S.Stolnik, M.C. Garnett, M.C. Davies et al. , *Coll. Surf.* 97 235-245, 1995
141. A.E. Hawley, L. Illum, S.S. Davis, *Pharm. Res.* 14(5) 657-661 , 1997
142. M. Tobio, R. Gref, A. Sanchez, R. Langer, M.J. Alonso, *Pharm. Res.* 15 (2) 270-275, 1998

143. H.M. Redhead, S.S Davis, L. Illum, J. Controlled Release 70 (3) 353-363, 2001
144. L. Mu, S.S. Feng, J. controlled Release 80 (1-3) 129-144, 2002
145. Y. W. Khin, S.S. Feng, Biomaterials 26(15), 2713-2722, 2005
146. Y. Tabata, Y. Ikada, Adv. Polymer Sci. 94 107-141, 1990
147. H. Suh, B. Jeong, f. Liu, s.W. Kim, Pharm. Res. 15 (9) 1495-1498, 1998
148. K.A. Foster, M. Yazdanian, K.L. J. Pharm. Pharmacol. 53 (1) 57-66, 2001
149. Sanjeeb K. Sahoo, Jayanth Panyam, Swayam Prabha, Vinod Labhasetwar, Journal of controlled release 82 105-114, 2002
150. Roy Bochm ALL, Zerrouk R, Ressi H. J Microencaps. 17: 195-205, 2000
151. Molpeceres J, Guzman M, Aberturas MR, Chacon M, Berges L. J Pharm Sci 85: 206-13, 1996
152. Chorny M, Fishbein I, Danenberg HD, Golomb G., J Control Rel 83: 389-400, 2002

PUBLICATION LIST

1. Internationally Refereed Journal Paper

1. Nanoparticles of Biodegradable Polymers for Chemotherapy across the Blood Brain Barrier (BBB) (in preparation)

2. International Conference papers

1. Chen Lirong, Yu Qianru, Wang Junping, Nanoparticles of biodegradable polymers to cross the blood brain barrier. 1st Nano-Engineering and Nano-Science Congress 2004, July 2004, Singapore

2. Chen Lirong, Yu Qianru, Feng Si Shen, Surface coating effects on nanoparticles of biodegradable polymers to cross the blood brain barrier. World Conference on Dosing of Antiinfectives, September 2004, Nurnberg, Germany

3. Yu Qianru, Chen Lirong, Feng Si Shen, Nanoparticles for Chemotherapy across the Blood Brain Barrier- Effects of Emulsifier and Particle Size. World Conference on Dosing of Antiinfectives, September 2004, Nurnberg, Germany